UNIVERSITY OF HELSINKI

DEPARTMENT OF PHYSICS

REPORT SERIES IN GEOPHYSICS
No 69

APPLICATION OF MAGNETIC, GEOCHEMICAL AND MICRO-MORPHOLOGICAL METHODS IN ENVIRONMENTAL STUDIES OF URBAN POLLUTION GENERATED BY ROAD TRAFFIC

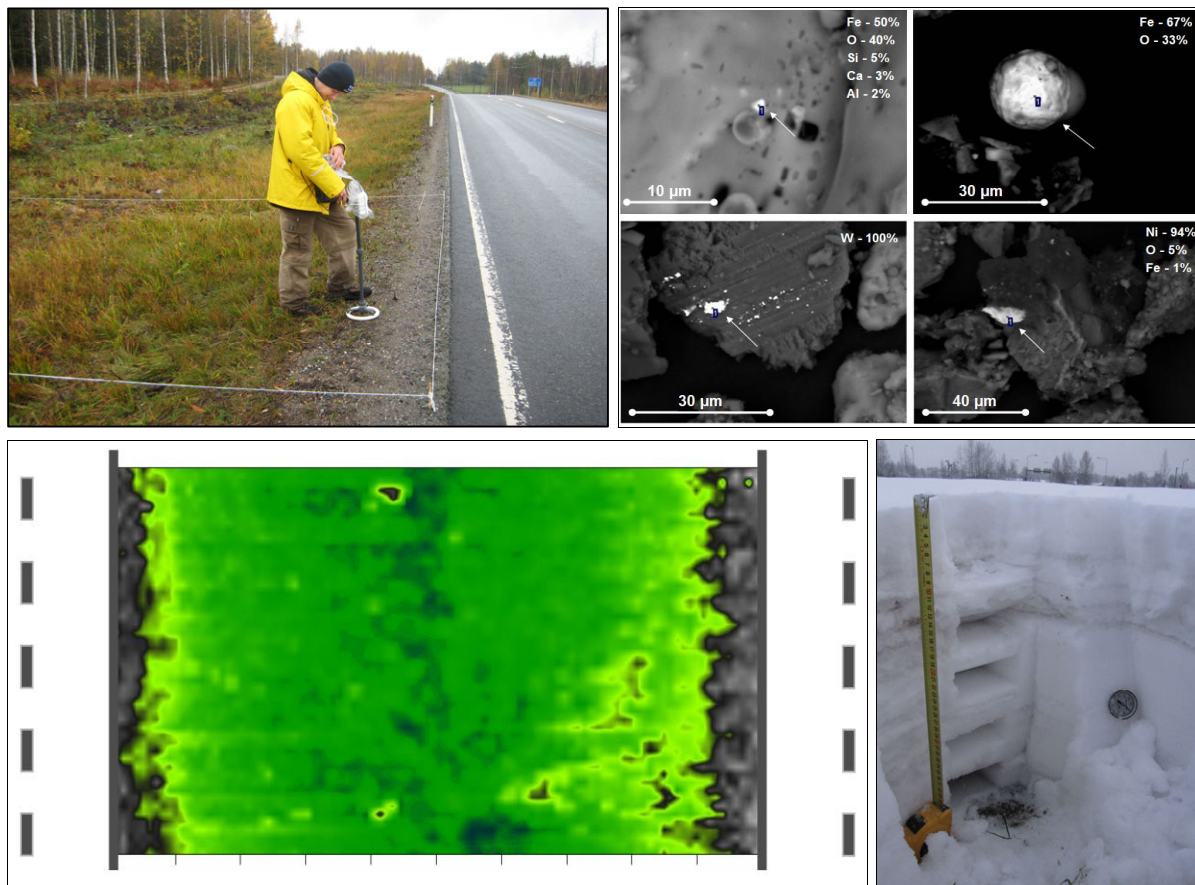Michał Stanisław Bućko

HELSINKI 2012

UNIVERSITY OF HELSINKI
DEPARTMENT OF PHYSICS

REPORT SERIES IN GEOPHYSICS
No 69

APPLICATION OF MAGNETIC, GEOCHEMICAL AND MICRO-MORPHOLOGICAL
METHODS IN ENVIRONMENTAL STUDIES OF URBAN POLLUTION GENERATED
BY ROAD TRAFFIC

Cover picture:
Top left: Magnetic susceptibility measurements of roadside topsoil near Mikkeli road no. 13 (southern Finland) using a Bartington MS2D susceptibility meter
Top right: Scanning Electron Microscopy (SEM) images with EDS (energy dispersive X-ray spectrometry) of vehicle-derived particles extracted from roadside snow
Bottom left: High-resolution 2D map of topsoil magnetic susceptibility (expressed in 10^{-5} SI) of the grass belt situated in the centre of motorway no. 45 (northern Helsinki)
Bottom right: Vertical snow profile taken near motorway no. 45. The picture shows characteristic "dark" layers indicating individual accumulation periods of road dust.

Michał Stanisław Bućko

HELSINKI 2012

Supervisors:

Associate Prof. Tadeusz Magiera
Institute of Environmental Engineering
Polish Academy of Sciences
Zabrze, Poland

Prof. Lauri J. Pesonen
Division of Geophysics and Astronomy
Department of Physics
University of Helsinki
Helsinki, Finland

Custos:

Prof. Karri Muinonen
Division of Geophysics and Astronomy
Department of Physics
University of Helsinki
Helsinki, Finland

Pre-examiners:

Dr Marcos A. E. Chaparro
National University of the Center of
Buenos Aires
Tandil, Argentina

Associate Prof. Daniela Jordanova
National Institute of Geophysics,
Geodesy and Geography
Bulgarian Academy of Sciences
Sofia, Bulgaria

Opponent:

Dr Karl W. J. Fabian
Geological Survey of Norway
Trondheim, Norway

APPLICATION OF MAGNETIC, GEOCHEMICAL AND MICRO-MORPHOLOGICAL METHODS IN ENVIRONMENTAL STUDIES OF URBAN POLLUTION GENERATED BY ROAD TRAFFIC

Michał Stanisław Bućko

ACADEMIC DISSERTATION IN GEOPHYSICS

To be presented, with the permission of the Faculty of Science of the University of Helsinki for public criticism in the Auditorium E204 of Physicum, Gustaf Hällströmin katu 2A, on November 10th, 2012, at 10:00 o'clock a.m.

Helsinki 2012

Table of contents

Abstract

Road traffic is at present one of the major sources of environmental pollution in urban areas. Magnetic particles, heavy metals and others compounds generated by traffic can greatly affect ambient air quality and have direct implications for human health.

The general aim of this research was to identify and characterize magnetic vehicle-derived particulates using magnetic, geochemical and micro-morphological methods. A combination of three different methods was used to discriminate sources of particular anthropogenic particles. Special emphasis was placed on the application of various collectors (roadside soil, snow, lichens and moss bags) to monitor spatial and temporal distribution of traffic pollution on roadsides.

The spatial distribution of magnetic parameters of road dust accumulated in roadside soil, snow, lichens and moss bags indicates that the highest concentration of magnetic particles is in the sampling points situated closest to the road edge. The concentration of magnetic particles decreases with increasing distance from the road indicating vehicle traffic as a major source of emission. Significant differences in horizontal distribution of magnetic susceptibility were observed between soil and snow. Magnetic particles derived from road traffic deposit on soil within a few meters from the road, but on snow up to 60 m from the road. The values of magnetic susceptibility of road dust deposited near busy urban motorway are significantly higher than in the case of low traffic road. These differences are attributed to traffic volume, which is 30 times higher on motorway than on local road. Moss bags placed at the edge of urban parks situated near major roads show higher values of magnetic susceptibility than moss bags from parks located near minor routes.

Enhanced concentrations of heavy metals (e.g. Fe, Mn, Zn, Cu, Cr, Ni and Co) were observed in the studied samples. This may be associated with specific sources of vehicle emissions (e.g. exhaust and non-exhaust emissions) and/or grain size of the accumulated particles (large active surface of ultrafine particles). Significant correlations were found between magnetic susceptibility and the concentration of selected heavy metals in the case of moss bags exposed to road traffic.

Low-coercivity magnetite was identified as a major magnetic phase in all studied roadside collectors (soil, snow, moss bags and lichens). However, magnetic minerals such as titanomagnetite, ilmenite, pyrite and pyrrhotite were also observed in the studied samples. The identified magnetite particles are mostly pseudo-single-domain (PSD) with a predominant MD fraction (>10 μm). The ultrafine iron oxides (>10 nm) were found in road dust extracted from roadside snow. Large magnetic particles mostly originate from non-exhaust emissions, while ultrafine particles originate from exhaust emissions.

The examined road dust contains two types of anthropogenic particles: (1) angular/aggregate particles composed of various elements (diameter ~1-300 µm); (2) spherules (~1-100 µm) mostly composed of iron. The first type of particles originates from non-exhaust emissions such as the abrasion of vehicle components, road surface and winter road maintenance. The spherule-shaped particles are products of combustion processes e.g. combustion of coal in nearby power plants and/or fuel in vehicle engines.

This thesis demonstrates that snow is an efficient collector of anthropogenic particles, since it can accumulate and preserve the pollutants for several months (until the late stages of

melting). Furthermore, it provides more information about spatial and temporal distribution of traffic-generated magnetic particles than soil. Since the interpretation of data obtained from magnetic measurements of soil is problematic (due to its complexity), this suggests the application of alternative collectors of anthropogenic magnetic particulates (e.g. snow and moss bags). Moss bags and lichens are well suited for magnetic biomonitoring studies, since they effectively accumulate atmospheric pollution and can thus be applied to monitor the spatio-temporal distribution of pollution effects.

Acknowledgements

This thesis is based on the following four papers, which are referred to in the text by their Roman numerals:

I.   Bućko, M.S., Magiera, T., Pesonen, L.J., Janus, B., 2010. Magnetic, geochemical, and microstructural characteristics of road dust on roadsides with different traffic volumes - case study from Finland. *Water Air and Soil Pollution* 209, 295-306.

II.   Bućko, M.S., Magiera, T., Johanson, B., Petrovský, E., Pesonen, L.J., 2011 Identification of magnetic particulates in road dust accumulated on roadside snow using magnetic, geochemical and micro-morphological analyses. *Environmental Pollution* 159, 1266-1276.

III.   Salo, H., Bućko, M.S., Vaahtovuo, E., Limo, J., Mäkinen, J., Pesonen, L.J., 2012. Biomonitoring of air pollution in SW Finland by magnetic and chemical measurements of moss bags and lichens. *Journal of Geochemical Exploration* 115, 69-81.

IV.   Bućko, M.S., Mattila, O.P., Chrobak, A., Johanson, B., Cuda, J., Tucek, J., Zboril, R., Pesonen, L.J., Leppäranta, M., 2012. Distribution of magnetic particulates in a roadside snowpack based on magnetic, microstructural and mineralogical analyses. *Submitted for publication to Geophysical Journal International (Wiley-Blackwell)*

Author's contribution to the publications

Paper **I**: Michał S. Bućko was the leading author of this publication. He conducted all the magnetic and SEM measurements at the University of Helsinki and combined these with the geochemical data acquired at the Institute of Environmental Engineering in Zabrze, Poland. He was responsible for data analysis and interpretation, writing the manuscript, and handling during the review and proof stage.

Paper **II**: Michał S. Bućko was the leading author of this paper. He performed all the magnetic and geochemical analyses at the University of Helsinki. For the purpose of this publication he conducted SEM analyses in cooperation with Geological Survey of Finland. He did most of the manuscript writing and was responsible for the manuscript handling during the review and proof stage.

Paper **III**: Michał S. Bućko and Hanna Salo (University of Turku) contributed equally to this work. Michał S. Bućko conducted the magnetic measurements including magnetic hysteresis, IRM, FORCs and temperature dependence of magnetic susceptibility as well as the processing of the geochemical data. He also wrote the general part of the manuscript and was responsible for the manuscript handling during the review process.

Paper **IV**: Michał S. Bućko was the leading author of this publication. He performed most of the magnetic measurements and was responsible for data analysis, interpretation, manuscript writing and handling during the review process.

1 Introduction

At present, issues concerning environmental quality in urban areas are of great importance since in several countries the majority of the population resides in urban complexes.

Urban air pollution originates from a wide variety of natural (biogenic) and anthropogenic sources. The first group includes forest fires, volcanic eruptions, pollen dispersal, evaporation of organic compounds and natural radioactivity. Mobile sources such as road (cars) and off-road vehicles (trains, ships and aircrafts) and stationary sources (power plants, manufacturing industries, waste deposits and burning facilities, household heating systems) are considered as main anthropogenic sources of pollution in urban areas.

These sources release various contaminants (e.g. heavy metals, particulate matter (PM), polyaromatic hydrocarbons (PAH)), which are deposited in urban, industrial, fluvial and maritime environments, thus posing serious risks to human health. Several studies have shown that long-term exposure to airborne pollutants, including those originating from road traffic, can lead to respiratory and cardiovascular diseases (Pope et al., 2002; Pope and Dockery 2006). According to the National Public Health Institute of Finland, as many as 2 million Finns suffer from occasional respiratory symptoms caused by airborne particles (Finnish Ministry of Transport and Communications, 2005). Moreover, it was estimated that around 200-400 Finns die prematurely every year because of air pollution. As the quality of the urban environment significantly influences human health, current environmental research is focused on spatial and temporal monitoring of anthropogenic pollutants.

Several studies have demonstrated that the impact of road traffic on the environment is accompanied by significant emissions of Fe-rich particles (Hoffmann et al., 1999, Matzka and Maher, 1999, Sagnotti et al., 2006), which are transported through atmospheric pathways and deposited in nearby surroundings. These pollutants can be easily detected due to their specific magnetic signature. The development of geophysical technology has enabled the application

of mineral magnetic methods in advanced studies of urban pollutants. Magnetic analyses are fast, non-intrusive and cost-efficient, thus they can be applied as a preliminary tool before the application of other time and cost consuming techniques. Since in many cases anthropogenic magnetic particles share an origin and existence with heavy metals (Beckwith et al., 1986; Goddu et al., 2004; Gautam et al., 2005a), magnetic techniques can be applied in order to trace urban pollution sources, together with geochemical analyses.

1.1 Vehicle emissions and their sources

Pollutants originating from road traffic can be grouped into two major types: exhaust and non-exhaust emissions. Exhaust emissions are produced during incomplete combustion of vehicle fuel which is a mixture of hydrocarbons and compounds improving combustion properties. During this process several types of pollutants are generated such as carbon monoxide (CO), nitrogen dioxide (NO_2), volatile organic compounds (VOCs), polycyclic aromatic hydrocarbons (PAHs) and particulate matter (PM). Incomplete combustion of fossil fuels as well as traffic-related suspension of road, soil and mineral dust leads to direct emission of various liquids and solids into the air (primary particles). Moreover, the gaseous substances released from exhaust systems, undergo gas-to-particle conversion (secondary particles) in the atmosphere (new particle formation by nucleation and condensation of gaseous precursors) (Pöschl, 2005). Secondary particles are mainly composed of inorganic compounds, including sulphates, ammonium and nitrates. Non-exhaust emissions are generated through mechanical (e.g. braking, clutch usage, tyre wear, road abrasion) and chemical processes (e.g. corrosion of vehicle elements).

Elements that have often been associated with vehicular emissions include Ba, Br, Ca, Cd, Co, Cr, Cu, Fe, Mg, Mn, Pb and Zn (Morawska and Zhang, 2002; Sternbeck et al., 2002; Lin et al., 2005; Lough et al., 2005). Birmili et al. (2006) concluded that materials rich in Cu, Ba and

Fe serve as an indication of abrasive vehicular wear, in particular brake linings. SEM and EDS analyses of brake linings and brake dust material generated during the application of brakes performed by Ingo et al. (2004) identified the presence of $BaSO_4$-containing particles in both brake lining material and break wear dust samples. The presence of Zn-containing particles may be attributed to the abrasion of tyres.

Exhaust and non-exhaust emissions can significantly contribute to the total mass of urban particulate matter ($PM_{2.5}$, PM_{10}). As reported by Ketzel et al. (2007) a large part (from 50 up to 85%) of the total PM_{10} emissions originates from non-exhaust emissions. In northern European countries, road sanding and the use of studded tyres are considered as major sources of the non-exhaust fraction of PM_{10}, which can account for up to 90% of airborne particulate matter (Forsberg et al., 2005; Omstedt et al., 2005).

1.2 Factors influencing emission of vehicle-derived pollutants

Several factors affect the emission of pollutants originating from road traffic. These include, but are not limited to:

- wide variety of vehicle (e.g. passenger cars, trucks, technology applied in particular vehicle brands) and engine types (e.g. diesel/gasoline-powered engine)
- vehicle use (e.g. number and duration of daily trips, number of cold starts) and quality of maintenance
- vehicle age
- fuel type and quality
- tyre type (e.g. friction/studded tyres)
- driving behaviour (e.g. aggressive/moderate driving)
- road conditions, capacity and quality of road infrastructure
- traffic conditions (e.g. heavy/light traffic)
- enforcements of inspection and maintenance programs or other emission control programs

- transportation planning (e.g. smoothing traffic flows on busy roads by active traffic management)
- weather conditions

This chapter describes only the influence of selected factors such as vehicle characteristics, driving conditions and application of different tyre types.

1.2.1 Vehicle characteristics (age, engine type)

Emission rates from motor vehicles depend on the year of manufacture and the type of used engine/fuel. Emissions from passenger cars differ significantly depending on the age of the vehicle. This is related with the development of new technologies by vehicle manufacturers, which constantly improve emission performance. One of the most crucial developments in the automotive industry was the application of catalytic converters, which significantly reduced the emission of toxic pollutants into the environment. However, catalytic converters are considered to be a major source of PGE (platinum group elements) pollution (Leśniewska et al., 2004).

Vehicles are mainly powered by combustion of fossil fuels (petroleum products). Diesel and petrol engines are at present the most common types of engines. These two engine types are a significant source of ultrafine PM. However, gasoline engines produce particles smaller in diameter than diesel engines. A significant portion of particles generated by diesel-powered engines have diameters smaller than 100 nm, while particles released from gasoline engines are less than 80 nm in diameter (Myung and Park, 2012). Moreover, particles from engines fuelled by compressed natural gas (CNG) or liquefied petroleum gas (LPG) are smaller than those from diesel emissions, with the majority between 20 and 60 nm in diameter. Diesel exhaust particles have been shown to display a multimodal size distribution (Kerminen et al., 1997) and are mainly carbonaceous agglomerates below 100 nm in diameter, while particles

generated by gasoline vehicles are also mainly carbonaceous agglomerates but considerably smaller, ranging from 10 to 80 nm (Morawska and Zhang, 2002).

Diesel-powered vehicles produce up to 100 times more PM than gasoline-driven ones (after Sagnotti et al., 2009 and references therein). Diesel vehicles generate 3–5 times higher amounts per km of most metals and trace elements (Geller et al., 2006). The pollutants mostly released by the diesel vehicles include elemental carbon (EC), light PAH (naphthalene, pyrene, phenanthrene), and metals such as Li, Be, Ti, Ni, Zn.

Particles from diesel and gasoline exhaust pipes show distinct compositional and magnetic hysteresis signatures (Sagnotti et al., 2009). The concentration of magnetic particles in dust samples collected from gasoline exhaust pipes is higher than in samples obtained from diesel-powered vehicles (Chaparro et al., 2010).

In the Helsinki metropolitan area, light duty vehicles constitute about 90% of all traffic, 80% of which are petrol vehicles and 20% diesel vehicles (Kauhaniemi, 2003).

1.2.2 Tyre type

In sub-arctic areas two types of winter tyres are used: friction and studded tyres. Friction tyres have a tread composed of a special rubber mixture and tread design with enhanced traction properties, while studded tyres are equipped with friction increasing hard metal tips. Studded tyres are more effective in enhancing vehicle traction under snowy and icy conditions, although this type of tyres is responsible for more intense wearing of the road surface, which results in increased concentrations of airborne PM during winter. Traction control with traction sanding and studded tyres enhances PM formation during the winter and the products accumulate in snow and ice in the road environment (Kupiainen, 2007). During springtime, when most of the snow and ice have melted and the surface becomes dry, the released

particles are again resuspended into the atmospheric surface layer by turbulences generated by passing vehicles, causing increased concentrations of urban particulate matter in the air.

At present the use rate of studded tyres is around 80% in Finland during the period from November to April (Kupiainen, 2007).

Other tyre properties such as its profile, pressure as well as vehicle mass and speed may also affect wear rates.

1.2.3 Driving conditions

Driving a motor vehicle includes four standard modes such as acceleration, cruising, deceleration, and idling. A single mode as well as the combination of driving modes ("driving behaviour") may produce different quantities of exhaust emissions. In other words, the emission rate from a particular vehicle depends on the way it is used. Frey et al. (2001, 2003) observed (1) higher vehicle emission rates during acceleration, with the largest emission rate observed when the vehicle was accelerated from a stop at a single intersection on a primary arterial road; and (2) the lowest emission rate during idling. Aggressive driving (e.g. rapid acceleration and braking, speeding) significantly increases fuel consumption compared to normal driving, which may result in higher emission levels (De Vlieger et al., 2000). The gender of the driver may have an influence on the driving behaviour. As reported by Ericsson (2000) men drive at higher average acceleration levels than women.

Both acceleration and braking enhance particle concentrations, but braking causes higher particle emissions than acceleration (Mathissen et al., 2012). Full stop braking performed during low and high speed can generate particles of different grain-size. As shown by Mathissen et al. (2011) the size distribution of 30 km h^{-1} full stop braking was unimodal with a mean particle size between 70 nm and 90 nm, while 100 km h^{-1} full stop braking size distributions were bimodal with a small mode near 10 nm and a second mode between 30 and 60 nm. It was suggested that the small particle mode most likely originated from brake wear

particles which were generated under heavy break loading. Furthermore, an exponential increase of the peak particle concentration with increasing velocity was found directly at the disc brake for full stop braking.

1.3 Dispersion of vehicle-derived particles

Particles deposited on or in the vicinity of the road, often referred to as road dust, may be re-entrained, or resuspended, into the air. The processes affecting road dust emissions are complex and depend on various environmental and meteorological factors.

The amount of material resuspended, due to traffic activity, is strongly dependent on particle size (Nicholson and Branson, 1990). As the size of particles increases, the rate at which particles fall due to gravity (the settling velocity, dry deposition) increases. Fine particles (diameter less than a few µm) may remain suspended in air indefinitely, while particles larger than about 20 µm settle rapidly and may not travel far from their sources of release (Sioutas, 2005).

The emission process of motor exhaust gas into the atmosphere generally involves cooling and dilution of aerosols, which may change their properties including particle number, size, surface area and chemical composition rapidly (Kittelson et al., 2000). During exhaust plume dilution, there is an evolving competition among new particle formation (nucleation mode), particle growth (condensation and coagulation mode) and reduction of particle size and mass (evaporation mode) (Canagaratna et al., 2010). Atmospheric dilution and coagulation play important roles in the rapid decrease of particle number concentration and the change in particle size distribution as the distance from the freeway increases (Zhu et al., 2002).

The initial dispersion depends on both traffic-induced and atmospheric turbulence. Exhaust emissions undergo two distinct dilution stages after being emitted. At first the released plume is diluted and moved from tailpipe to roadside by the strong turbulence generated by passing

vehicles, and then moved again from the roadside to the ambient air by atmospheric turbulence induced by wind and atmospheric instability (Zhang et al., 2004). Speed and weight/size of the vehicle may have an influence on the strength of atmospheric turbulence near the road as well as the degree of resuspension. Heavy duty vehicles (e.g. buses and trucks) trigger high peaks in wind velocity affecting resuspension of road dust. Moreover, some studies indicated a linear increase of emissions with vehicle speed on unsurfaced roads (for review, see Kupiainen, 2007).

During vehicle movement the force of the wheels causes pulverization of materials deposited on the road surface. Particles are lifted and dropped from the rolling wheels, and the road surface is exposed to strong air currents in turbulent shear with the surface. The turbulent wake behind vehicles continues to act on the road surface after they have passed. The on-road measurements performed by Mathissen et al. (2012) indicated the lowest emissions on motorways, where the highest average velocity was noticed. The authors explain that high velocity traffic removes the road dust from the road surface or keeps it suspended in the air. However, Zhu et al. (2002) reported that total particle number concentrations increased with increasing wind speed. Moreover, total particle number concentrations are also related to traffic density and decrease significantly during traffic slowdown.

Resuspension of road dust is additionally influenced by humidity, precipitation (wet deposition), temperature, solar radiation and the condition of the road surface. It has been observed that road dust emissions are low during periods with wet surfaces (Kuhns et al., 2003). During rainy and melting periods the amount of deposited road dust may decrease as part of the particles is washed out from the road surface with runoff waters. Some studies have shown that intensive rain events can significantly reduce the surface loading of roads (Bris et al., 1999; Vaze and Chiew, 2002).

1.4 Magnetic mineral and domain types

Five major groups of magnetic materials are recognized:

Diamagnetism is exhibited by substances with no unpaired electrons in the various electron shells of their constituent atoms. Diamagnetic behaviour is only exhibited when an external (natural or artificial) magnetic field is applied; under such conditions the electron orbits become aligned so as to oppose the external field. This alignment of orbital planes, which would otherwise cancel, therefore produces a magnetic moment. When the field is removed this induced moment is lost and electron orbits precess, effectively at random, to positions giving no net magnetic moment. This type of magnetic behaviour is fundamental to all substances, but is weak and negative (relative to the direction of the applied field), and becomes masked if other types of magnetic behaviour are present. Diamagnetic substances are e.g. water, quartz, feldspar, calcite, kaolinite.

Paramagnetism arises due to the interactions of unpaired electrons in partially filled orbitals. Due to these interactions, paramagnetic materials (e.g. siderite, biotite, and pyrite) have a net magnetic moment due to the partial alignment of magnetic moments in the direction of the applied field. As in diamagnetism, removal of the external field causes the magnetization to return to zero due to electron spin moments and orbital moments cancelling each other out. The magnetization of paramagnetic material is generally one or two orders of magnitude larger than the diamagnetic one, but is still weak.

Ferromagnetic materials, such as iron (Table 1), cobalt, and nickel have atomic moments that exhibit very strong interactions (due to exchange forces) and result in parallel alignment of atomic moments. This parallel alignment produces a large net magnetization, even in the

absence of an applied field, giving rise to a spontaneous, or intrinsic, magnetization and a remanent magnetization can be retained.

Antiferromagnetism. In an antiferromagnet, magnetic spins are aligned antiparallel, which results in a material with no net magnetic moment. An example of this type of material would be one in which there are two sublattices of magnetic atoms with equal but oppositely directed moments. This could be brought about by equal numbers of atoms with the same moment in each sublattice, or unequal numbers with moments such that the oppositely directed moments balance. Since antiferromagnetic materials (e.g. hematite, goethite) have an uneven number of electrons, they can acquire a permanent magnetization, or remanence, after exposure to a magnetic field.

Spin-canted (anti)ferromagnetism is a condition when antiparallel magnetic moments are deflected from the antiferromagnetic plane, resulting in a weak or parasitic magnetism. Hematite is an example of a canted antiferromagnet (Table 1).

Ferrimagnetic materials (e.g. magnetite, greigite, pyrrhotite, Table 1) have antiparallel spin alignments that result from super-exchange forces (where the exchange coupling force extends over an intermediate anion). This causes the electron spins in adjacent cations to be reversed, creating two oppositely magnetized, but intimately mixed lattices within the material. Since ferrimagnetic materials have an uneven number of electrons, they can acquire a permanent magnetization, or remanence, after exposure to a magnetic field.

The so-called **domains** arise due to competition between magnetic forces within the material and are produced by an attempt to minimize the overall energy state of the magnetic grain (Dunlop and Özdemir, 1997). In general, large grains can accommodate multiple domains

(multidomain, MD), while smaller grains can only accommodate one domain (single domain, SD). Large SD grains and small MD grains, which have some SD-like properties, are referred to as pseudo-single domain (PSD) grains.

Superparamagnetic (SP) grains are so small that they cannot support a stable domain configuration: upon a change in external field the spin configuration conforms to the new situation rapidly (on a laboratory timescale) (Dekkers, 2007).

Table 1. Magnetic properties of selected minerals (Carmichael, 1989; Dunlop and Özdemir, 1997; Dekkers, 2007).

Mineral	Composition	$T_{V, M, INV} (C°)$	$T_{C, N} (C°)$	Hc (mT)	Ms (kAm^{-1})	Magnetic structure
Magnetite	Fe_3O_4	-153	580	5-80	480	Ferrimagnetic
Titanomagnetite	$Fe_{3-x}Ti_xO_4$		150-540		125	Ferrimagnetic
Maghemite	γFe_2O_3	<250	590-675	5-80	380	Ferrimagnetic
Hematite	αFe_2O_3	-15	675	100-500	~2.5	Canted-antiferromagnetic
Pyrrhotite	Fe_7S_8	(-240)	320	8-100	~80	Ferrimagnetic
Goethite	$\alpha FeOOH$		120	>1000	~2	Antiferromagnetic
Iron	αFe		765	<1-10	1715	Ferromagnetic
Greigite	Fe_3S_4		~330	15-40	~125	Ferrimagnetic

T_V– Verwey transition, T_M – Morin transition, T_{INV} – Inversion temperature, T_C – Curie temperature, T_N –Neel temperature, Hc – coercivity, Ms – saturation magnetization.

1.5 Application of magnetic analyses in traffic pollution studies

In the past years, magnetic techniques have been used to determine the levels, extent, and sources of atmospheric pollution in many urban and industrial areas (Hoffmann et al., 1999; Muxworthy et al., 2001; Hanesch and Scholger, 2002; Jordanova et al., 2010). These techniques are based on the fact that urban dust contains a relatively high concentration of magnetic minerals, mainly in the form of iron oxides, derived from fossil fuel combustion

(industrial, domestic and vehicular), industrial emissions and re-deposition of abrasion/erosion products (both mineral/crustal and anthropogenic). Magnetic analyses have been successfully applied to identify and delineate high-polluted areas in urban environments (Charlesworth and Lees, 2001; Moreno et al., 2003; Gautam et al., 2004; Goddu et al., 2004; Shilton et al., 2005; Kim et al., 2007). Several studies have also shown a correlation between magnetic parameters and meteorological data (Morris et al., 1995; Muxworthy et al., 2001, 2003; Spassov et al., 2004) and geochemical data (Morris et al., 1995; Robertson et al., 2003; Spassov et al., 2004; Lu et al., 2005; Kim et al., 2007) and Tomlinson Pollution Load Index (PLI) (Lu et al., 2007; Canbay et al., 2010).

Magnetic susceptibility of air filters was shown to be correlated to the mutagenic potency of polycyclic aromatic compounds (PAC) and the pollutants SO_2 and NO_2 (Morris et al., 1995). McIntosh et al. (2007) revealed a well-defined relationship between isothermal remanent magnetization (IRM) and concentration of total nitrogen oxides (NO_x) in the city of Madrid, and suggested that the magnetic signal is associated with traffic-related emissions.

Magnetic particles derived from vehicle emissions are of variable shapes and their magnetic properties are dominated by Fe_3O_4 (Sagnotti et al., 2009; Chaparro et al., 2010), but pure Fe particles were also found in street dust (Hopke et al., 1980; Kim et al., 2007). Combustion processes produce both magnetic spherules and the aggregates (Muxworthy et al., 2001; Moreno et al., 2003; Shilton et al., 2005; Maher et al., 2008), while abrasion/corrosion generates mostly magnetic aggregates (Kim et al., 2007; Maher et al., 2008).

A number of techniques have been applied by researchers to sample urban dust. Vacuum cleaners were used to collect urban dust samples from gutters, playgrounds and directly from road surfaces (Olson and Skogerboe, 1975; Hopke et al., 1980; Ng et al., 2003). Another common and simple technique is sweeping with a polyethylene dustpan and brush (Xie et al., 1999; Charlesworth and Lees, 2001; Robertson et al., 2003; Gautam et al., 2004; Shilton et

al., 2005; Kim et al., 2007, 2009; Chaparro et al., 2010; Marié et al., 2010; Yang et al., 2010). Charlesworth and Lees (2001) collected atmospheric fallout by placing sheets of sticky backed plastic film at sites around Coventry City, UK, whilst Flanders (1994) used sticky tape wrapped around a pole or tree. Vehicle-derived particulates can also be collected from the inner walls of exhaust pipes by using plastic scrapers (Lu et al., 2005; Sagnotti et al., 2009; Chaparro et al., 2010; Marié et al., 2010) or from wheel rims and the inside of engine hoods using clean paper directly on the exposed surfaces (Sagnotti et al., 2009).

In the literature several different techniques have been described to collect PM samples for magnetic studies; for example filter methods (e.g. Morris et al., 1995; Xie et al., 2000; Muxworthy et al., 2001, 2003; Spassov et al., 2004; Shilton et al., 2005; Sagnotti et al., 2006; Maher et al., 2008), collecting street dust (Xie et al., 1999, 2000; Chaparro et al., 2010), soils (Hoffmann et al., 1999), and vegetation samples including tree bark (Flanders, 1994; Kletetschka et al., 2003), leaves (Matzka and Maher, 1999; Moreno et al., 2003; Davila et al., 2006; McIntosh et al., 2007; Sagnotti et al., 2009) and needles (Urbat et al., 2004). Table 2 presents a review of selected publications reporting the use of various techniques for sampling urban dust generated by road traffic.

Table 2. Review of literature (selected papers) reporting the use of various techniques for sampling urban dust generated by road traffic.

References	Studied material and area	Rock-magnetic parameters	Other analyses/parameters
SOIL			
Olson and Skogerboe, 1975	Urban roadside soils and street dust samples collected from three distinct geographic areas in Colorado, Missouri, Chicago		Magnetic separation, gradient density, XRD, chemical analysis: Pb, microscopic observations, emission spectrography
Hoffmann et	Roadside soil along a major	κ_{is}, χ, IRM, low-field	

al., 1999	road in SW Germany	susceptibility vs. temperature, M_s vs. temperature	
Hanesch and Scholger, 2002	Soils collected from urban (various sampling sites: parks, residential areas, road sections, playgrounds for children) and industrial areas in Austria	χ	Chemical analysis: As, Cd, Co, Cr, Cu, Hg, Mo, Ni, Pb, Pt, Se, V, Zn
Amereih et al., 2005	Soil samples along two Austrian motorways	χ	Chemical analysis: Sb
Gautam et al., 2005a	Soil samples collected from the following areas in Kathmandu, Nepal: suburban background site, recreational areas and parks situated in core urban areas, recreational park close to an industrial area.	χ, IRM, SIRM, SIRM/χ ratio, χ vs. temperature	Chemical analysis: Cd, Cu, Co, Cr, Mn, Ni, Pb, Zn, Fe, PLI
Lu and Bai, 2006	Soils collected from industrial, roadside, residential, campus areas and public parks located around Hangzhou City, China	χ_{lf}, χ_{hf}, $\chi_{fd\%}$, IRM, SIRM, HIRM, magnetization parameter ($F_{300\,mT}\%$)= [$100 \times$ (IRM$_{300\,mT}$ / SIRM)], S_{-100}, IRM$_{20\,mT}$, ARM	X-ray diffractometer XRD, chemical analysis: Cu, Zn, Cd, Pb
Lu et al., 2007	Urban topsoil from within Luoyang City, China. Samples collected from: industrial, roadside, residential, green recreation areas, parks and commercial centres	χ_{lf}, χ_{hf}, $\chi_{fd\%}$, IRM, SIRM, S_{-100mT}, HIRM, IRM$_{20mT}$, hysteresis parameters, magnetic susceptibility vs. temperature	Chemical analysis: Fe, Mn, Cd, Cr, Cu, Pb, Zn, XRD, PLI
Yang et al., 2007	Urban soil samples collected from: industrial areas, villages, a main road with heavy traffic and roads around the East Lake in Wuhan, China	χ_{lf}, χ_{hf}, $\chi_{fd\%}$, ARM, IRM, SIRM, S_{-300}, χ vs. temperature	Chemical analysis: Co, Cr, Cu, Mn, Ni, Pb, Zn, PLI
El-Hasan, 2008	Urban roadside topsoils of Sahab city, Jordan	χ_{in}, M_s	
El-Hasan et al., 2009	Urban topsoil samples collected across the whole of Sahab city, Jordan	χ_{in}, M_s	Chemical analysis: Fe, Mn, Cu, Co, Cr, Ni, Zn, Cd and Pb,

XRD, IP

Canbay et al., 2010	Topsoil samples collected from the Izmit Gulf coastal area, Turkey: industrial, roadside, park, green, residential and commercial areas	χ_{lf}, χ_{hf}, $\chi_{fd\%}$	Chemical analysis: Cu, Pb, Zn, Ni, Cr, Cd, Co, PLI

BIOMONITORS

Matzka and Maher, 1999	Roadside tree leaves of birch (*Betula pendula*) collected in the city centre, suburbs, and along the rural coast of Norwich, England	IRM_{300mT}, AF demagnetization	
Moreno et al., 2003	Leaves collected from different tree species situated near urban parks and high traffic roads in Rome, Italy	χ, IRM, SIRM, S_{-300}, SIRM/χ	
Urbat et al., 2004	Pine (*Pinus nigra*) needles collected in parks, residential areas and near major roads, railways, the airport and industrial complexes in Cologne, Germany	κ, χ, ARM, IRM, H_{CR}, S_{-300}, SIRM, SIRM/ARM, IRM/κ, temperature-dependence of magnetic susceptibility	SEM with EDX, chemical analysis: Fe
Gautam et al., 2005b	Three types of tree leaves obtained from cypress (mainly *Cupressus corneyana*), silky oak (*Grevillea robusta*), and bottlebrush (*Callistemon lanceolatus*), sampled along road corridors and recreational parks in both urban and suburban areas of Kathmandu, Nepal	χ, IRM	Chemical analysis: Cd, Cu, Co, Cr, Fe, Mn, Ni, Pb, Zn, SEM with EDS
Davila et al., 2006	Tree leaves obtained from London Plane (*Platanus hispanica)* in urban and sub-urban areas of the coastal city of Vigo, Spain	$SIRM_{1T}$, S_{-300}	SEM with EDXRA, chemical analysis: Cd, Cr, Cu, Fe, Mn, Ni, Pb, Zn
McIntosh et al., 2007	Tree leaves of Hybrid Plane (*Platanus x hispanica)*	κ, IRM_{1T}, S_{-300mT}, S_{-100mT}, IRM_{1T}/κ, H_{CR}	

	collected in a central, urban area of Madrid, Spain: roadside, plaza and park locations		
Szönyi et al., 2008	Tree leaves of evergreen oak (*Quercus ilex)* collected in Rome, Italy, at sites with different traffic conditions (e.g. urban parks, intersections with very high traffic)	κ, χ, IRM, H_{CR}, hysteresis parameters, ARM, χ_{ARM}, temperature-dependence of magnetic susceptibility	SEM with EDS

FILTERS

Morris et al., 1995	PM_{10} filters collected at two air quality monitoring stations located in urban areas of Hamilton, Canada	κ	PAC polycyclic aromatic compound, NO_2, SO_2, O_3 SEM, electron microprobe analysis, bioassay
Muxworthy et al., 2001	PM_{10} and PM_{70} filters collected at two permanent stations located in areas of high traffic congestion, Munich, Germany. One station is in the city centre and one in the city suburbs	m_S, M_S, H_C, magnetization vs. temperature	Ozone, benzene, toluene, *o*-dimethylbenzene, CO, NO, NO_2, SO_2, SEM with EDX
Muxworthy et al., 2002	Two self-constructed PM fallout collectors were placed at different distances from the street, Munich, Germany	Hysteresis parameters, rotational hysteresis, magnetic susceptibility/magnetization vs. temperature	Mössbauer spectroscopy, SEM with EDX
Muxworthy et al., 2003	PM_{10} filter samples collected at two permanent air monitoring stations located in the city centre and suburbs of Munich, Germany	SIRM, SIRM AF_{25}/SIRM AF_{10} ratio	CO, NO, NO_x ($NO+NO_2$), SO_2
Spassov et al., 2004	PM_{10} filter samples (high-volume air sampler) collected in Zürich, Switzerland, at sites with different exposures to pollution sources (e.g. urban park in the city centre, motorway tunnel, semi-rural region	ARM, χ_{ARM}	

Sagnotti et al., 2006	PM$_{10}$ filters collected at six air-monitoring stations distributed within Rome, Italy, at sites with different traffic conditions, varying from urban park to high-traffic industrial area	κ, χ, ARM, hysteresis parameters, FORCs, IRM, H$_{CR}$, S$_{-300}$, S$_{-100}$, thermal demagnetization of M$_{RS}$, $\chi_{fd\%}$	

URBAN DUST

Hopke et al., 1980	Road dust from Urbana, Illinois, USA		Magnetic separation, gradient density, chemical analysis: Sb, As, Ba, Br, Ca, Cd Ce, Cs, Cr, Co, Dy, Eu, Ga, Hf, Fe, La, Pb, Lu, Mn, Hg, Ni, K, Rb, Sm, Sc, Se, Ag, Na, Sr, Tb, Th, U, Yb, Zn, Zr
Xie et al., 1999a	Street dust from street gutters and pavements in the city of Liverpool, UK. The sampling sites were distributed over diverse locations: pedestrian streets, gardens and roads with different traffic densities	χ_{lf}, χ_{hf}, $\chi_{fd\%}$, ARM, χ_{ARM}, SIRM$_{1T}$, IRM$_{20mT}$, IRM$_{-20mT}$, IRM$_{-300mT}$, SOFT, HIRM, χ_{HIGH}, χ_{ARM}/SIRM, SOFT%, HARD%, (SIRM-IRM$_{-20mT}$), (SIRM-IRM$_{-300mT}$), χ_{HIGH}/χ_{lf}	
Xie et al., 2001	Street dust samples obtained from street gutters and pavements in the city of Liverpool, UK. The sampling sites were distributed over diverse locations: pedestrian streets, gardens and roads with different traffic densities, covering the whole city centre	χ_{lf}, χ_{hf}, $\chi_{fd\%}$, χ_{ARM}, SIRM$_{1T}$, IRM, ARM, IRM$_{-20mT}$, IRM$_{-300mT}$, SOFT, HIRM, SOFT%, HARD%, χ_{ARM}/SIRM	organic matter content measured by LOI, X-ray fluorescence (XRF): Si, Ti, Ca, K, Fe, S, Pb, Rb, Sr, Zn, Zr
Ng et al., 2003	Playground dust, Hong Kong. Most urban playgrounds are located close to major traffic routes	χ_{lf}, χ_{hf}, $\chi_{fd\%}$, NMR Natural Remanent Magnetization, ARM, SIRM, HIRM, S$_{-300}$, ARM/SIRM	Chemical analysis: Zn, Cu, Cd, Cr, Pb, Mn, Fe, organic carbon contents
Robertson et al., 2003	Urban sediment from inner and outer city road surfaces	SIRM, SIRM/χ, S$_{-100mT}$, χ_{lf}, χ_{hf}, $\chi_{fd\%}$	Chemical analysis: Fe, Cu, Zn, Pb, Mn,

	in Manchester, UK		organic matter content based on LOI, SEM
Goddu et al., 2004	Road dust from an industrial area in Visakhapatnam city, India	κ, $\kappa_{fd\%}$, SIRM, IRM, hysteresis parameters, FORCs, temperature-dependence of κ	SEM with EDX
Lu et al., 2005	Vehicle emission particulates collected from the inner wall of exhaust pipes in Hangzhou City, China	χ_{lf}, χ_{hf}, $\chi_{fd\%}$, IRM, SIRM, ARM, HIRM, IRM_{20mT}	Chemical analysis: Cu, Cd, Pb, Fe
Shilton et al., 2005	Street dust collected from three roads (two urban and one residential road) in the West Midlands, UK.	χ_{lf}, χ_{hf}, $\chi_{fd\%}$, ARM, χ_{ARM}, IRM, χ_{ARM}/SIRM, SIRM/χ, ARM/χ, S-ratio, HIRM, SIRM	Organic matter content based on LOI, SEM
Kim et al., 2007	Roadside dust collected in the city of Seoul, Korea, from industrial and high traffic sites (e.g. in a tunnel, on a bridge nearby the railway station)	χ, ARM, SIRM, IRM, S_{-300}, temperature-dependence of magnetic susceptibility	SEM with EDS, chemical analysis: Cr, Cu, Fe, Mn, Pb, Zn
Kim et al., 2009	Roadside dust collected at industrial, park, residential and traffic areas in Seoul, Korea	χ, ARM, SIRM, M_s, IRM, S_{-300}, χ vs. temperature	SEM with EDS
Yang et al., 2010	Road dust samples collected from an industrial area, villages, a main road with heavy traffic and roads around the East Lake in Wuhan, China	χ_{lf}, χ_{hf}, $\chi_{fd\%}$, ARM, IRM, SIRM, hysteresis parameters, H_{CR}, χ_{ARM}/χ_{lf}, ARM/χ_{lf}, χ vs. temperature	Chemical analysis: Fe, Cu, Pb, Zn, Mn, Co, V, Ni, Cr, PLI

COMBINATION OF TECHNIQUES

Flanders, 1994	Airborne particulates collected from various surfaces and directly from the atmosphere (e.g. spider webs, tree trunk and leaves, fly ash from oil and coal combustion, road dust)	Magnetization	SEM
Xie et al., 2000	Street dust from street gutters and pavements. The	χ_{lf}, χ_{hf}, $\chi_{fd\%}$, χ_{ARM}, $SIRM_{1T}$, IRM, ARM,	organic matter content measured by

	dust sampling sites were distributed over diverse locations: pedestrian streets, gardens and roads with different traffic densities. Topsoil samples were collected from roadsides, gardens or waste land in Liverpool, UK.	IRM_{-20mT}, IRM_{-300mT}, SOFT, HIRM, SOFT%, HARD%, χ_{HIGH}, χ_{HIGH}/χ_{lf}, $\chi_{ARM}/SIRM$	LOI
Charlesworth and Lees, 2001	Urban dusts and sediments from lakes, streams, streets and wetlands sampled in Coventry, UK	χ_{lf}, SIRM	
Kletetchka et al., 2003	Samples of soil and tree bark (*Red Maple*, *Acer rubrum*) collected along a major motorway, Washington DC, USA	SIRM, hysteresis parameters, κ	
Gautam et al., 2004	Soil, sediment and road dust samples collected from urban and suburban areas in Kathmandu, Nepal	κ_{is}, χ, IRM, χ vs. temperature	SEM with EDS
Maher et al., 2008	Urban roadside tree leaves of birch (*Betula pendula*), air filter samples (high-volume air sampler) in Norwich, UK	SIRM	Chemical analysis: Fe, Pb, Zn, Mn, Ba, Cd, Cr, SEM with EDXA
Mitchell and Maher, 2009	Leaves of lime trees (*Tilia platyphyllos*) collected within the perimeter of the city ring road, background and suburban areas in Lancaster, UK. In addition, air PM_{10} filters (high-volume air sampler) collected from each sampled tree location	χ_{ARM}, IRM, ARM, SIRM, HARD%, $\chi_{ARM}/SIRM$ ratio, temperature dependence of IRM	SEM with EDX
Sagnotti et al., 2009	Tree leaves of evergreen oak (*Quercus ilex*) collected along a high-traffic square and a large green park in Rome, Italy. In addition, material collected from exhaust pipes of gasoline and diesel engines, wheel rims around disk brakes,	Hysteresis parameters, IRM, H_{CR}, FORCs, $\kappa_{fd\%}$, temperature dependence of κ	SEM with EDS

	engine hoods and filters at an automatic air monitoring station on a high-traffic road		
Chaparro et al., 2010	Samples collected from exhaust pipes of gasoline and diesel vehicles, brake systems, roadside sediments and soils, Buenos Aires, Argentina	κ, ARM, IRM, χ, κ_{ARM}, κ_{ARM}/κ ratio, SIRM, S$_{-300}$, H$_{CR}$, SIRM/κ ratio	SEM with EDS, chemical analysis: Li, K, Na, Mg, Ca, Sr, Ba, Cr, Mn, Fe, Co, Ni, Cu, Al, Zn, Cd, Pb, PLI
Marié et al., 2010	Samples collected from exhaust pipes of gasoline and diesel vehicles, brake systems, roadside sediments and soils, asphalt material, Buenos Aires, Argentina	κ_{is}, κ, ARM, IRM, κ_{ARM}, κ_{ARM}/κ ratio, SIRM, S$_{-300}$, H$_{CR}$, SIRM/κ ratio, thermal demagnetization of magnetic susceptibility and remanent magnetisation	Chemical analysis: Li, K, Na, Mg, Ca, Sr, Ba, Cr, Mn, Fe, Co, Ni, Cu, Al, Zn, Cd, Pb , SEM with EDS

χ mass-specific magnetic susceptibility; χ_{lf} low frequency mass-susceptibility; χ_{hf} high frequency mass-susceptibility; $\chi_{fd\%}$ frequency dependent magnetic susceptibility; κ volume magnetic susceptibility; ARM anhysteretic remanent magnetisation; IRM isothermal remanent magnetisation; κ_{ARM} anhysteretic susceptibility; SIRM saturation of IRM; S-ratio, (S$_{-300}$) (-IRM$_{-300mT}$/SIRM$_{1T}$); S-ratio, (S$_{-100}$) (-IRM$_{-100mT}$/SIRM$_{1T}$); H$_{CR}$ remanent coercivity; SEM scanning electron microscopy; EDS energy dispersive spectroscopy; EDXRA energy dispersive X-ray analysis; χ_{in} initial magnetic susceptibility; M$_S$ saturation magnetization; XRD X-Ray diffraction; IP Index of Pollution; PLI Tomlinson Pollution Load Index; κ_{is} in situ magnetic susceptibility; χ_{ARM} susceptibility of anhysteretic remanent magnetization; EDX energy dispersive X-ray; EDXA energy-dispersive X-ray analysis; m$_S$ saturation moment; H$_C$ coercive force; LOI loss-on-ignition; soft IRM, SOFT=[(SIRM-IRM$_{20mT}$)/2]; hard IRM, HIRM [=(SIRM-IRM$_{-300mT}$)/2]; χ_{HIGH} high-field susceptibility; SOFT%=[100×SOFT/SIRM]; HARD%=[100xHIRM/SIRM]; FORC First Order Reversal Curves; AF Alternating Field.

1.6 Aims of the study

Three main objectives were defined for this dissertation. The first objective was to identify and characterize magnetic vehicle-derived particulates using magnetic, geochemical and micro-morphological methods. A combination of three different methods was used in order to obtain data that can provide information on possible sources (e.g. exhaust, non-exhaust) of specific particles.

The second objective was to monitor the spatial and temporal distribution of traffic pollution on roadsides with different traffic volumes. Data displaying the spreading mechanisms and

dispersal patterns of vehicle-generated particles into the environment may support future urban planning to better protect the environment and human health.

The third objective concerns the application of various collectors (soil, snow, lichens and moss bags) in detailed studies of urban traffic pollution.

Screening of topsoil magnetic properties serves as a rapid, efficient and inexpensive technique to determine the degree of environmental pollution. This reduces the need for extensive geochemical analysis. Mosses and lichens accumulate large amounts of trace metals, thus these bioaccumulators can be successfully used in monitoring airborne trace element pollution. Although mosses and lichens are widely used in atmospheric pollution studies, few results have so far been published about their suitability for enviro-magnetic research. Winter is the longest season in Finland, lasting for about 100 days in the south-western part and 200 days in Lapland (northern Finland). During this period, permanent snow cover occurs in most of the areas. Since snow acts as a natural filter for various chemical elements and particles, and its sampling is easy and can be performed during several months, it can be effectively used in detailed studies of various anthropogenic pollutants and their sources. This thesis focuses on testing the suitability of snow in monitoring the distribution of vehicle-derived magnetic particles.

Four different collectors of urban dust were analysed during three distinct seasons (soil in summer, snow in winter, moss bags and lichens in spring and summer) in order to study their effectiveness in spatio-temporal magnetic monitoring of traffic pollution.

2 Materials and methods

2.1 Study sites and sampling

Four different collectors were used in this research project: roadside soil, snow, lichens and moss bags (Fig. 1). Roadside soil and snow (Figs. 1A, B, **Papers I, II, IV**) were collected from two sites located near a busy urban motorway (Tuusula no. 45, northern Helsinki, site 1) and a low traffic road (Mikkeli no. 13, south-eastern Finland, site 2) (Fig. 2). Site 1 is located in an urban area with heavy traffic (>60 000 cars per day), while site 2 is situated in an area surrounded mostly by forest, where road traffic can be considered as the only anthropogenic activity (traffic volume <2000 cars per day). The speed limit at sites 1 and 2 is 100 km h^{-1} and 80 km h^{-1}, respectively. Six shallow soil profiles from site 1 and four from site 2 were taken up to a depth of 14 cm (Fig. 1A, **Paper I**). In each profile, samples were collected from the following depths: 0–1, 7–8, and 13–14 cm. It is important to note that the sampling points of roadside soil were selected on the basis of magnetic susceptibility mapping using a Bartington MS2 susceptibility meter with a D field loop sensor.
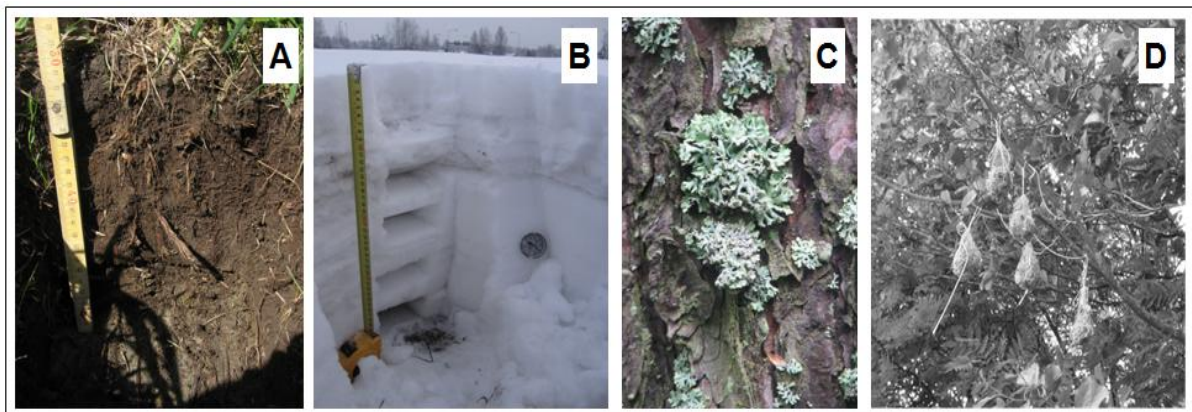
*Figure 1. Profile of roadside topsoil near a busy urban motorway (A). An example of a vertical snow profile examined at sampling site 1. The picture shows characteristic "dark" layers indicating individual accumulation periods of road dust (B). Epiphytic lichen Hypogymnia physodes on a tree trunk (C). Moss bags placed on a tree at a height of ~3 m (D) (**Papers I, III, IV**).*

Figure 2. Map of the study area (southern Finland) showing the sampling locations: (1) a busy urban motorway in northern Helsinki; (2) a low traffic road near Mikkeli; (3) Turku area.

Surface snow samples (top 7 cm) were collected in January and March 2009 at sites 1 and 2, respectively (**Paper II**). Sampling was carried out along four parallel profiles at site 1 and three near site 2. The sampling points were located at the following distances from the road edge: 5, 10, 15, 20, 25, 30, 40, 50 and 60 m at site 1 and 5, 7, 9, 11, 13, 15, 20, 25, 30 and 40 m at site 2. At each sampling point, ~400 cm^3 of fresh snow was collected. Four snow samples with a volume of ~2400 cm^3 were collected from each site for heavy metal analyses. All samples were transported from the field directly to the laboratory in portable travel coolers. A total of 74 snow samples were obtained from both sites. In the laboratory, the samples were melted at room temperature and after complete evaporation of the water the remaining material was used for the analyses.

Vertical snow profiles were taken at site 1 during the winter season 2010-11 (Fig. 1B, **Paper IV**). The snow profiles were excavated during four sampling campaigns: 7th December 2010, 20th January 2011, 2nd March 2011 and 6th April 2011. During each sampling campaign

observations were made at the same spots located at 5 m, 10 m and 15 m from the road edge. Bulk snow samples (whole snow column down to the soil surface) with a volume of 1500 cm^3 were collected from each profile and stored in plastic bags (3×500 cm^3). Furthermore, individual snow layers were distinguished at each snow profile on the basis of the physical properties of the snow (density, grain size, temperature and stratification) and characteristic dark layers, which indicated individual accumulation periods of road dust (Fig. 1B). From each layer, a snow sample of 1500 cm^3 volume was collected and stored in plastic bags (3×500 cm^3). A total of 140 snow samples were collected during the whole winter season. All samples were transported from the field directly to the laboratory in portable cool boxes at temperature below $0°$ C. Similarly as in **Paper II** the snow samples were melted at room temperature and after complete evaporation of the water the remaining material was used for analysis.

Samples of epiphytic lichen *Hypogymnia physodes* (Fig. 1C) were collected randomly from 116 sites distributed throughout Turku (site 3, Fig. 2, **Paper III**). At each sampling point, three subsamples were collected from 0.5 to 2 m height and from at least two sides of each trunk. In the laboratory, lichens were dried at T<40 °C and crushed using a plastic knife and agate mortar. The lichen samples were used to produce a map of magnetic susceptibility distribution of the Turku area (presented in **Paper III**). Twenty lichen samples were selected from the areas with the highest magnetic susceptibility ("hotspots") for detailed magnetic analyses from which four representative samples were selected for chemical analysis. One sample taken from the forest was selected as the background. Moreover, at site 3 the moss bags (composed of moss *Sphagnum papillosum*, Fig. 1D) were exposed to airborne pollution at 22 sampling points: along major roads with high traffic (n=7) and in three urban parks (Kupittaa n=5, Urheilupuisto n=5 and Puolalanpuisto n=3) situated mostly near minor roads with low traffic. The traffic routes in the Turku area were classified into two groups: major

roads (>10,000 vehicles per day) and minor roads (<10,000 vehicles per day). Five moss bags were placed at each sampling point on trees at a height of 2.5–3 m (Fig. 1D). The bags were collected from site 3 in 2010 after 87–88 days of exposure. To determine background levels of studied pollutants, one set of moss bags was placed at a control site (Kemiö Island, ~50 km SE of Turku). The moss bag samples from site 3 and control area were collected in polyethylene bags and transported to the laboratory. Subsamples from each sampling point were combined into one composite sample. The moss material was dried to constant weight at T<40 °C and homogenized. Samples were ground into a fine powder in a swing mill equipped with an agate-grinding vessel. The resultant material was used for magnetic and chemical analysis.

2.2 Methods

2.2.1 Volume and mass-specific magnetic susceptibility

Magnetic susceptibility specifies the ability of material to acquire magnetization when subjected to external magnetic field. Volume magnetic susceptibility is defined as the magnetization (*M*) acquired per unit field (*H)*,

$$\kappa = M/H \qquad (1)$$

In SI units *M* and *H* are measured in A/m, thus κ is dimensionless. The measured magnetic susceptibility is generally expressed as mass-specific susceptibility, which is calculated from the following equation,

$$\chi = \kappa/\rho \qquad (2)$$

where ρ is the density of material.

The values of χ are given in m^3kg^{-1}. The magnetic susceptibility of diamagnetic material is negative. Water is considered as a very strong diamagnet ($\chi = -0.90 \times 10^{-8} m^3kg^{-1}$), as are

minerals such as quartz and calcite (Evans and Heller, 2003). Paramagnetic materials exhibit slightly positive susceptibility.

Magnetic susceptibility reflects the concentration, grain-size, and type of magnetic minerals present in a sample. A high value of magnetic susceptibility indicates a high concentration of magnetic minerals (Maher, 1986; Thompson and Oldfield, 1986). Specimens such as soil or road dust usually are a composite of diamagnetic, paramagnetic, and ferro/ferrimagnetic contributions. Ferro/ferrimagnetic materials have very high magnetic susceptibilities so that for concentrations larger than ~1% the measured susceptibility may be equated to the ferromagnetic susceptibility. In the case of lower concentrations the paramagnetic and diamagnetic contributions can be substantial (Dekkers, 2007).

In environmental studies, magnetic susceptibility is a very convenient parameter since virtually all materials can be measured and the measurement is simple and fast (typically a few seconds). The measurements are also non-destructive and can be made in the laboratory as well as in the field (Evans and Heller, 2003). This means that magnetic susceptibility measurements can be used as a primary tool for mapping of spatial and temporal distribution of pollutants and identification of their sources, before other time and cost consuming techniques such as analytical chemistry or geochemistry need to be applied.

For the purpose of this research project the following magnetic susceptibility meters were used:

1. Bartington MS2 susceptibility meter with two sensors: MS2B and MS2D (**Paper I, III**)

The MS2B is a portable laboratory sensor which accepts 10 cm^3 samples in plastic holders. It has the ability of performing measurements of κ at two different frequencies (0.46 and 4.6 kHz). The MS2D loop sensor has a diameter of 18.5 cm and it is used directly in the field. This sensor is applied in surface measurements (top 10 cm) of soils, rocks, stream channels etc.

2. Agico KLY-3S kappabridge (**Paper I, II, III, IV**)

The KLY-3S kappabridge operates at a frequency of 875 Hz and a field intensity of 300 Am^{-1} RMS.

3. ZH instruments SM-100 (**Paper IV**)

The SM-100 sensor measures magnetic susceptibility at five fixed frequencies (0.5-8 kHz) and six field strengths (10-320 A/m). In this study, the κ measurements were performed at a frequency of 506 Hz and a field intensity of 80 A/m.

2.2.2 Frequency dependent magnetic susceptibility

This parameter is obtained from magnetic susceptibility measurements performed at two different frequencies: low (κ_{lf}) and high (κ_{hf}). Measurements made at these two frequencies are generally used to detect the presence of ultrafine (<0.03 μm) superparamagnetic (SP) minerals in samples. Samples where SP minerals are present will show slightly lower values when measured at high frequency; samples without superparamagnetic minerals will show identical κ values at both frequencies (Dearing, 1999). Frequency dependent susceptibility is mostly expressed as a percentage of the mass-specific frequency dependent susceptibility:

$$\chi_{fd\%} = (\chi_{lf} - \chi_{hf})/\chi_{lf} \times 100 \qquad (3)$$

Low-frequency (χ_{lf}) and high-frequency (χ_{hf}) mass-specific susceptibilities are calculated according to equation 2 from κ_{lf} and κ_{hf} values, respectively. Table 3 shows values of $\chi_{fd\%}$ indicating the presence of SP particles in the sample.

Table 3. Interpretation of $\chi_{fd\%}$ values (according to Dearing, 1999).

Low $\chi_{fd\%}$	<2.0	Virtually no SP grains
Medium $\chi_{fd\%}$	2.0-10.0	Mixture of SP and coarser grains, or SP grains < 0.05 μm
High $\chi_{fd\%}$	10.0-14.0	Virtually all SP grains
Very high $\chi_{fd\%}$	>14.0	Erroneous measurement, anisotropy, weak sample or contamination

2.2.3 Temperature dependence of magnetic susceptibility

Temperature dependent magnetic susceptibility (κ-T) is a measurement which describes variations of κ across a range of temperatures; from liquid nitrogen (-200 °C, Fig. 3) up to several hundred degrees Celsius. This method is widely used in paleo-, rock- and enviromagnetic studies for identification of magnetic minerals in analysed samples.

The temperature variations of κ are not observed in diamagnetic minerals such as quartz, feldspars and calcite. However, ferro, ferri and antiferromagnetic minerals can be identified at certain temperatures by so-called Verwey (T_V) and Morin (T_M) transitions, and Curie(Tc)/Neel(T_N) point observed during low and high κ-T measurements, respectively (Table 1).

Low temperature dependence of magnetic susceptibility

Measurement of low κ-T allows the identification of magnetic minerals such as magnetite and hematite. The presence of magnetite is indicated by T_V, which occurs at about -150 °C (Fig. 3) and marks a change in the crystallographic distribution of the iron cations such that the previously cubic framework is slightly distorted to monoclinic symmetry (Evans and Heller, 2003). However, T_V indicates only the contribution of stoichiometric magnetite. The presence of non-stoichiometric (substituted) magnetite such as titanomagnetite cannot be recorded by low κ-T curves. At T_M (-15° C, Table 1) hematite undergoes changes in magnetic properties, where it loses spin canting, and hence weak ferromagnetism (Evans and Heller, 2003).
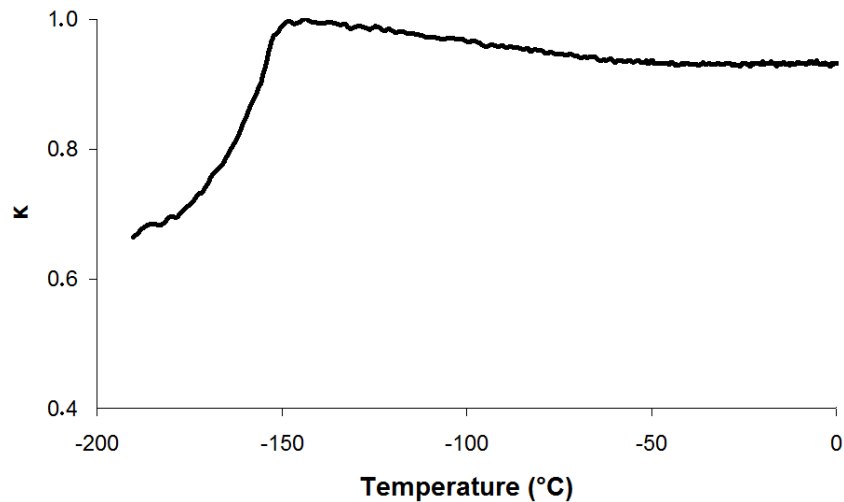
*Figure 3. Low-temperature behaviour of magnetic susceptibility (κ in 10^{-6} SI normalized by max. value) of roadside topsoil (0-2 cm) collected near the edge of a motorway, showing Verwey transition for magnetite at -150° C (**Paper I**).*

High temperature dependence of magnetic susceptibility

High κ-T curves indicate the presence of ferrimagnetic and antiferromagnetic minerals such as magnetite, titanomagnetite, pyrrhotite and hematite by Curie (Tc)/Neel(T_N) temperature (Table 1) when the susceptibility decreases acutely reflecting a transition to a paramagnetic state (Hrouda et al., 2003). The interpretation of data obtained from high-temperature experiments is more problematic than in the case of low-temperature curves. Heating of magnetic minerals often leads to their destruction and formation of new mineral phases. This applies especially to various paramagnetic minerals (e.g. pyrite, clay minerals) and the presence of organic matter within the sample, which creates reducing conditions that favour the growth of magnetite (France et al., 1999).

In this study, κ-T at low (-200 °C) and high (700 °C) temperatures was measured using an AGICO KLY-3S kappabridge in conjunction with a CS-3/CS-L furnace. During low κ-T experiments liquid nitrogen was applied to obtain a temperature of -200 °C. **Papers I-IV** include only κ-T curves measured at low temperatures.

2.2.4 Magnetic hysteresis parameters, First Order Reversal Curves

Hysteresis parameters are used to identify specific magnetic mineralogies, grain sizes and concentrations within samples. Parameters such as saturation magnetization (in Am^2), saturation remanent magnetization (M_{RS}, in Am^2)and coercivity (in T) are obtained from hysteresis data (Fig. 4A). The previous chapter (2.2.1) described magnetic susceptibility, which expresses the ability of a material to acquire M while H is being applied. This is referred to as induced magnetization (Evans and Heller, 2003). Diamagnetic and paramagnetic materials lose M when H is removed. A different situation is observed in the case of ferro and ferrimagnets. When a strong positive H is applied ferro and ferrimagnetic materials become magnetically saturated and acquire M_S. As H decreases to zero, M does not fall to the origin. After complete removal of H ferro and ferrimagnetic materials acquire M_{RS}. If a negative H is applied, M gradually falls to zero and then reverses and eventually saturates again (Fig. 4A).

A remanent magnetization acquired by exposure to a field at ambient temperature is an isothermal remanent magnetization. If the applied H is sufficient to saturate IRM, we obtain saturation isothermal remanent magnetization, which is equivalent to M_{RS} (Evans and Heller, 2003). Since particular magnetic minerals saturate at different applied fields, these can be identified in the studied samples by the distribution of IRM curves (Fig. 4B). Together with IRM measurements D.C. (direct current) demagnetization of SIRM is performed in order to obtain coercivity of remanence. IRM curves are measured on previously demagnetized samples by applying a positive H which is removed and the remanence is measured. This procedure is repeated stepwise for larger fields until saturation is reached. D.C. demagnetization curves (Fig. 4B) are obtained by saturating the samples in a positive H followed by stepwise measurement of the remanence after application of progressively increasing negative H.
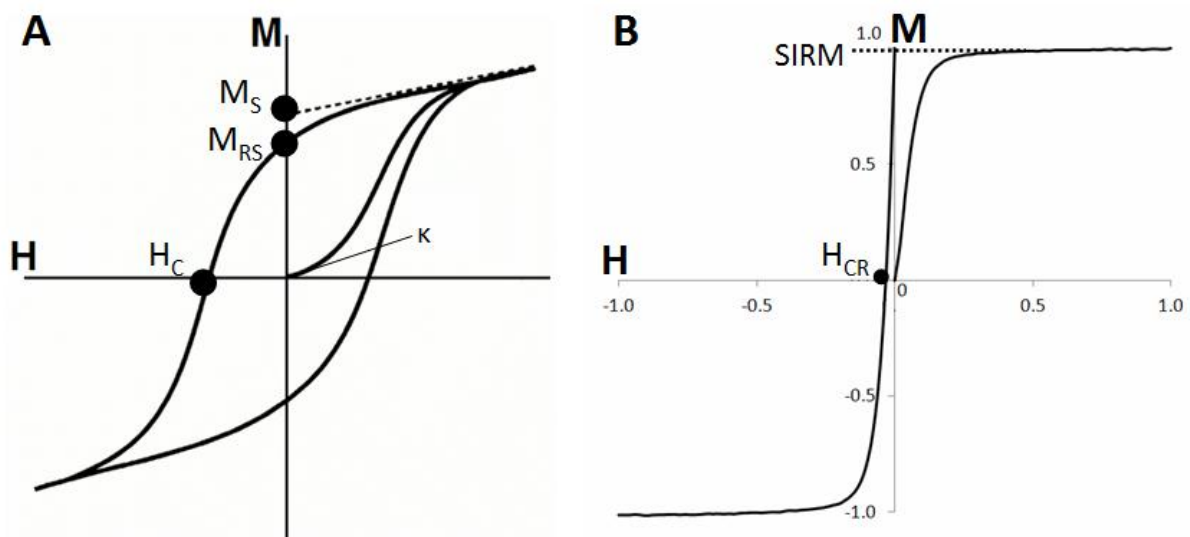
*Figure 4. Example of a hysteresis loop. M_S - saturation magnetization; M_{RS} - saturation remanent magnetization; H_C - coercivity; κ - initial susceptibility; M - magnetization (Am^2); H - magnetic field (T) (A). Isothermal remanent magnetization (IRM) acquisition curve and D.C. (direct current) demagnetization of saturation IRM (SIRM) indicating the presence of magnetite in a lichen sample collected near the road (**Paper III**). H_{CR} - coercivity of remanence; M - magnetization (Am^2 kg^{-1}) normalized by max. value; H - magnetic field (T) (B).*

Magnetic parameters of hysteresis are helpful for discrimination of specific magnetic grain sizes when plotted in a Day diagram (Fig. 5) (Day et al., 1977). It is possible to distinguish magnetic grains such as MD, PSD, SD, and SP using the ratios M_{RS}/M_S and H_{CR}/H_C.

M_{RS}, which is equivalent to SIRM, is a ferrimagnetic concentration-dependent parameter and similarly as χ it can indicate the amount of magnetic material within samples.

Magnetic grain size variations in samples of uniform mineralogy can be characterized by the SIRM/χ ratio. The ratio decreases with increasing magnetic grain size for magnetite grains of sizes larger than 1 μm (Peters and Dekkers, 2003).

Ferro and ferrimagnetic materials have lower values of H_C than antiferromagnetic materials (magnetite: 5–80 mT, hematite: 100–500 mT). Minerals with low coercivity values are termed magnetically "soft" while those with high values are "hard" (Dekkers, 2007).

The shape of a hysteresis loop determines the magnetic properties of the studied material. The height of the loop is a function of the concentration and type of the magnetic mineral, while the width of the loop is entirely controlled by the "hardness" of the mineral. Low-coercivity minerals such as magnetite and pyrrhotite produce steep and narrow loops, while hematite is characterized by a broader loop.
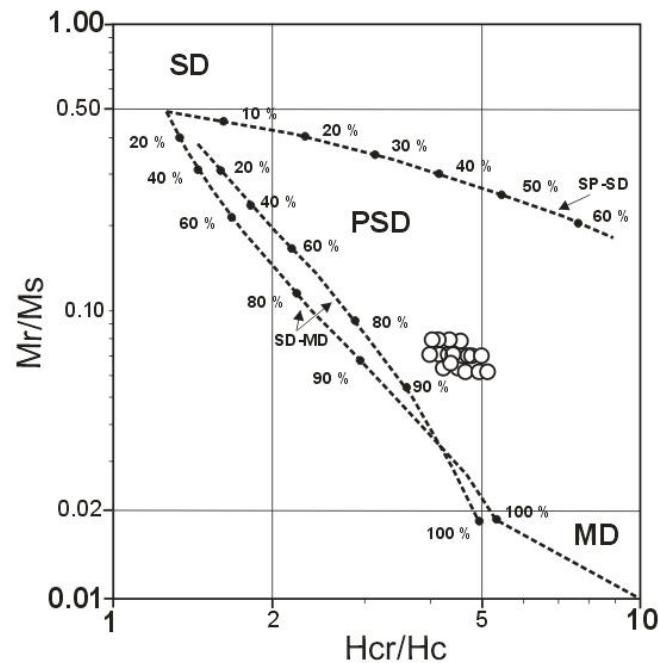

*Figure 5. Day plot for road dust accumulated on roadside snow sampled near a busy urban motorway. Boundaries for single-domain (SD), pseudo-single-domain (PSD) and multi-domain (MD) grains and mixing lines, indicated by broken lines (SD/MD and SD/superparamagnetic (SP) grains), are shown after Dunlop (2002) (**Paper II**). The diagram shows that the road dust contains PSD type magnetic grains.*

A FORC (First Order Reversal Curves) diagram (Fig. 6) is produced from a class of partial hysteresis curves known as FORCs. A FORC is obtained after the sample magnetization is saturated in a large positive applied field. The field is then decreased to a smaller or negative field, H_a, and the FORC is defined by measuring the magnetization $M(H_a, H_b)$ of the sample when the field H_b is gradually increased from H_a to the saturating field. A FORC distribution is obtained from the mixed second derivative. A FORC diagram provides a detailed characterization of coercivity distribution of the magnetic particles, their size distribution and

magnetic interactions. A detailed description of the method can be found in Roberts et al. (2000).

In this study, a Princeton Measurements Co. Vibrating Sample Magnetometer (VSM) model 3900 was used to determine hysteresis loops, FORCs and IRM curves at room temperature using a maximum field of 1 T (**Papers I-IV**). FORC diagrams were produced using FORCAM, a MatLab code written by Michael Winklhofer (Winklhofer and Zimanyi, 2006).
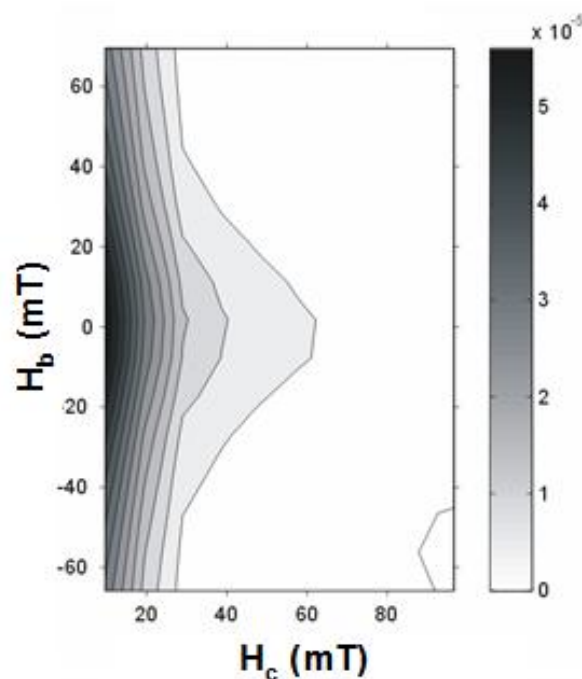
*Figure 6. FORC (First Order Reversal Curves) diagram of selected lichen sample collected near one of the major roads in Turku, Finland (**Paper III**). The diagram indicates the presence of multi-domain (MD) magnetic grains in the sample. H_b - bias or magnetic interaction; H_C - coercivity distribution.*

2.2.5 Scanning Electron Microscopy

Scanning electron microscope (SEM) images the surface of solid specimen by application of a beam of high-energy electrons. These electrons possess significant amounts of kinetic energy, which is dispersed as a variety of signals generated by electron-sample surface interactions, when random electrons are decelerated on the surface of solid sample.

Signals derived from electron-sample surface interactions provide information about sample morphology (texture), chemical composition, crystalline structure and mineral orientation (Goldstein et al., 2003). Spatial variations of these properties with respect to selected areas of the surface of the sample are displayed in a 3-dimensional image (Fig. 7).

Types of signals produced by SEM include:

- secondary electrons: produce SEM images, show morphology and topography of the sample surface

- backscattered electrons (BSE): illustrate contrasts in composition in multiphase samples

- diffracted backscattered electrons (EBSD): determine crystal structure and orientation of minerals

- photons: characteristic X-rays, which describe composition and the abundance of elements in the sample, and continuum X-rays

- visible light (cathodoluminescence) and heat

Areas ranging from approximately 1 cm to 5 µm in width can be studied using SEM (magnification ranging from 10X to approximately 100,000X). SEM is capable of analysing selected point locations in the sample using two types of X-ray spectrometers: energy-dispersive (EDS), which is able to measure the complete X-ray energy spectrum simultaneously, and wavelength-dispersive spectrometer (WDS), which can measure only one wavelength (one element at a time) (Hounslow and Maher, 1999). Analysis using EDS determines the qualitative and semi-quantitative chemical composition of the surface of the samples.

Nonconductive specimens examined by SEM need to be coated with a thin film of conducting material. The most common coatings are gold and carbon.

In this study (**Papers I-IV**), we used a SEM model JEOL JSM5900 LV equipped with an energy dispersive X-ray spectrometer (EDS) with INCA Feature phase detection and classification software provided by Geological Survey of Finland. The INCA Feature

software performs automatic scans of the sample area and detects grains using backscattered electron imaging (recording size, shape and grey level) and subsequently analyses and classifies the phases by EDS.
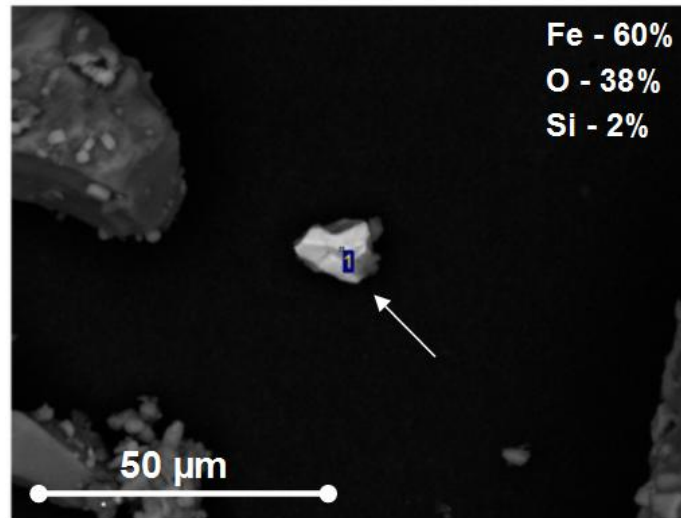

*Figure 7. Example of an SEM image and chemical composition (based on EDS spectra) of a magnetite particle identified in roadside snow collected near a busy urban motorway (**Paper II**).*

2.2.6 Geochemical analyses

Magnetic analyses can be successfully used in detailed studies of airborne pollutants. However, in order to discriminate the sources of these pollutants other analyses (e.g. geochemistry, electron microscopy) are required to complement the magnetic characterisations. Since the magnetic measurements are fast and cost-effective, and can be effectively used in monitoring the spatial and temporal changes in air pollution, these methods can be applied as a preliminary tool to select representative sampling locations for geochemical analyses. Furthermore, this multidisciplinary approach allows for a better characterization of different pollutants and a better understanding of the relationship between different polluting species (e.g. magnetic particles, heavy metals).

In order to investigate the correlation between magnetic and geochemical data the concentration of selected heavy metals was determined using the following methods:

*Table 4. Geochemical analyses performed in this research (**Papers I-III**).*

	Analysed material	Methodology	Extracted heavy metals
Paper I	roadside soil	Atomic absorption spectrophotometry (AAS) after extraction in aqua regia according to ISO 11466 procedure	Fe, Mn, Pb, Zn, Cd, Cu, Cr, Ni, Co
Paper II	road dust extracted from roadside snow	AAS after dissolution in a mixture of concentrated H_2SO_4/HF/HNO_3	Fe, Mn, Pb, Zn, Cd, Cu, Cr, Ni, Co
Paper III	moss bags and lichens exposed to road traffic	Inductive coupled plasma (ICP) atomic emission spectroscopy (ICP-OES, Jobin-Yvon Ultima 2) and mass spectrometry (ICP-MS, Agilent 7500ce) according to SFSEN ISO 11885 and 17294	Fe, Mn, Pb, Zn, Cd, Cu, Cr, Ni, Co, Al, As, Ba, Ca, Mo, Na, Ti, V

Trace element enrichment can be estimated from the Tomlinson Pollution Load Index (PLI) (**Paper III**). The PLI indicates how much a sample exceeds the heavy metal concentrations of natural environments and give an indication of the overall toxicity status of a sample. The PLI (Angulo, 1996) is a measure of central tendency, defined as the nth root of the multiplication of the concentration factors (CF_{metal}):

$$CF_{metal}=C_{metal}/C_{background} \qquad (4)$$

$$PLI={}^{n}\sqrt{(CF1 \times CF2 \times CF3 \times \ldots CFn)} \qquad (5)$$

where CF_{metal} is the ratio between the concentration of each heavy metal (C_{metal}) to the corresponding background concentration ($C_{background}$) obtained from the reference site or the lowest concentration value detected for each heavy metal. According to Singh et al. (2003) PLI values vary from 0 (unpolluted) to 10 (highly polluted). A PLI below 1 indicates that elemental loads are near the background level, and above 1 indicates the extent of pollution.

2.2.7 Additional analyses

Paper IV includes data obtained from the following measurements:

Table 5. Additional analyses performed in this research project.

Methodology	Instrument
Low (2 to 300 K) temperature magnetic measurements	Superconducting Quantum Interference Device (SQUID) magnetometer (XL-7, Quantum Design)
Mössbauer measurements at 14 K and room temperature in zero magnetic field	Mössbauer spectrometer with a ^{57}Co(Rh) source of γ-rays
X-ray powder diffraction (XRD) pattern	PANalytical X'Pert PRO MPD diffractometer (CoK$_{\alpha}$ radiation) in the Bragg-Brentano geometry, equipped with an X´Celerator detector and programmable divergence and diffracted beam anti-scatter slits
Wavelength dispersive X-ray fluorescence spectrometry (WD-XRF)	S4 Pioneer (Bruker AXS) spectrometer

3 Summary of the results

Road dust accumulated in roadside soil, snow, lichens and moss bags exposed to road traffic was examined using magnetic, geochemical and micro-morphological analyses. The results of these studies are presented in **Papers I**, **II**, **III** and **IV**.

The spatial distribution of magnetic susceptibility of road dust accumulated in roadside soil, snow, moss bags and lichens indicates the highest values at the measurement points situated closest to the road edge (**Papers I-IV**) (Figs. 8, 9). κ and χ decrease with increasing distance from the road edge. The decreasing trend of magnetic susceptibility of road dust with increasing distance from the road clearly indicates vehicle traffic as a major source of emission of magnetic particles. Most of the pollutants are deposited near the road and this is

indicated by the highest values of κ and χ. The decrease in concentration and grain size of magnetic particles in soil and tree leaves with increasing distance from the road indicates vehicle traffic as a significant source of magnetic particles emissions (Hoffmann et al., 1999; Moreno et al., 2003). However, there are clear differences in horizontal distribution of magnetic susceptibility between soil (**Paper I**) and snow (**Paper II**) (Figs. 8, 9). Magnetic particles derived from road traffic deposit within a few meters distance from the road on soil and up to 60 m on snow. However, it is difficult to interpret the data obtained from soil measurements due to the contribution of its "background" to the total value of magnetic susceptibility.
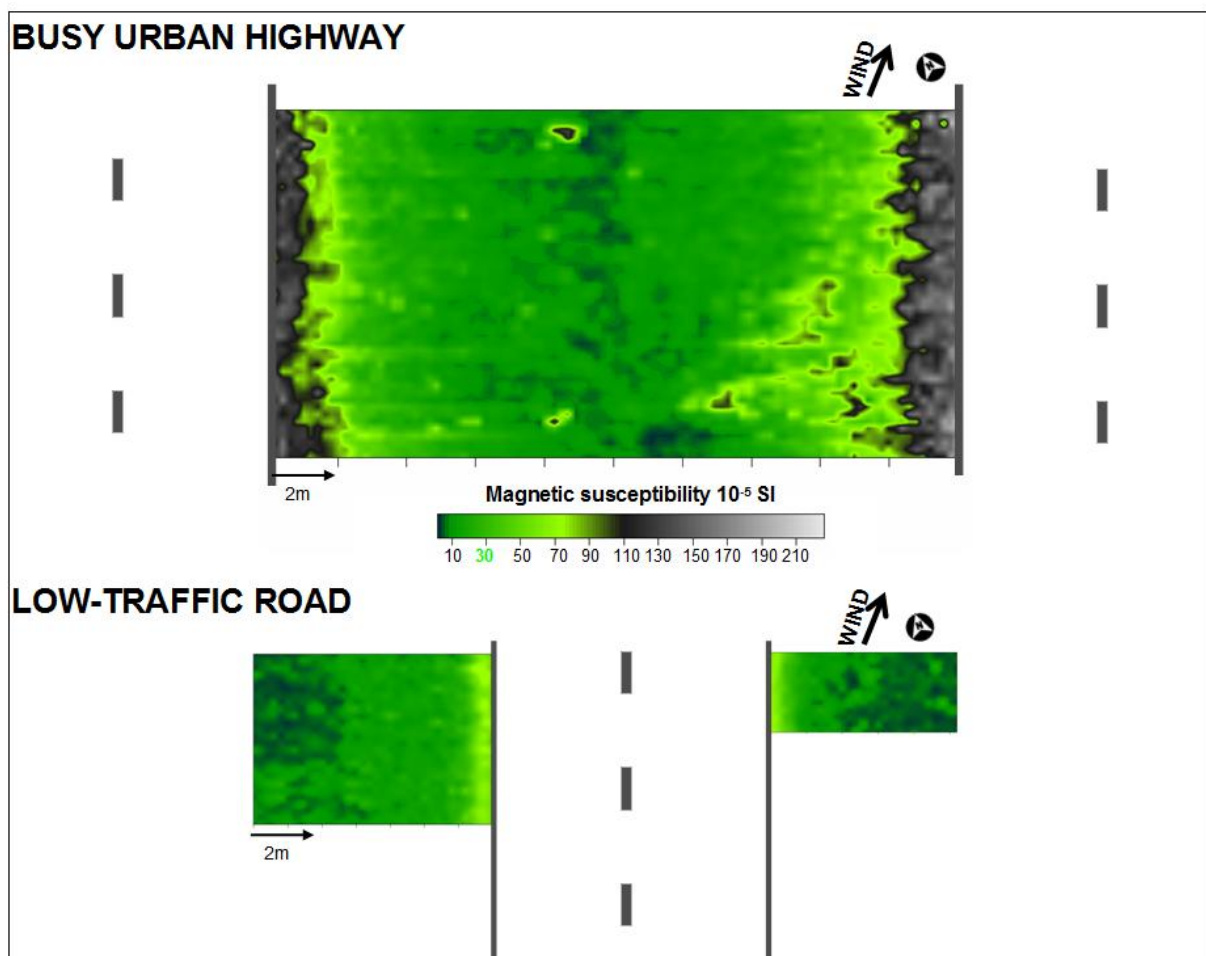

*Figure 8. High-resolution 2D maps of topsoil magnetic susceptibility measured near busy urban motorway and low-traffic road (modified from **Paper I**).*

The differences in magnetic susceptibility data obtained from both collectors might be due to the fact that accumulation of urban PM on snow occurs seasonally and represents short time periods (days, months), while soil, if not covered by snow, can accumulate pollutants over several decades (years). Moreover, the soil and snow samples were collected in different seasons of the year (soil in summer, snow in winter). As reported by Kim et al. (2007) magnetic concentrations and magnetic particle sizes exhibit systematic seasonal fluctuations (high and large in winter versus low and small in summer) due to the seasonal influx variations of anthropogenic magnetic materials.
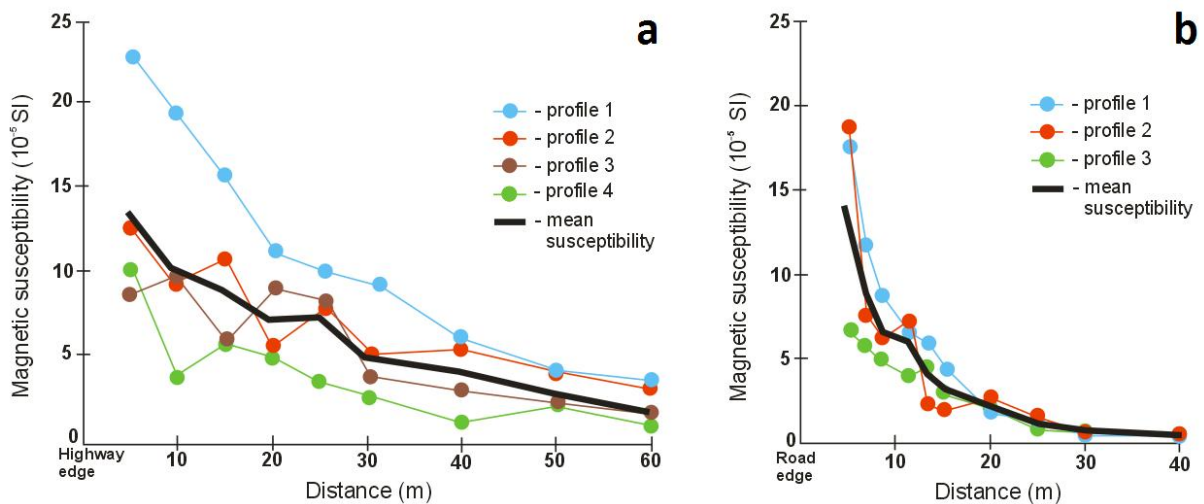

*Figure 9. Profiles of magnetic susceptibility of road dust accumulated on snow located near a busy urban motorway (a) and low-traffic road (b) (modified from **Paper II**).*

More intensive dispersion of magnetic particles occurs near the busy urban motorway than near the low-traffic road (**Papers I and II**, Figs. 8, 9). This is attributed to traffic volume, which is 30 times higher on the motorway than on the local road. However, deposition rate of vehicle-derived particles at certain sites may also be controlled by other factors such as topography, meteorological (e.g., precipitation, temperature, wind direction and speed) and driving conditions (e.g., speed, acceleration and braking) (Chapter 1.2).

As described in **Paper III**, the moss bags placed at the edge of urban parks situated near major roads show higher values of χ than the moss bags from parks located near minor routes.

Moreover, the lowest χ was noticed in the centre of the urban parks (~250 m from the road). Matzka and Maher (1999) observed minimal values of magnetic remanence for birch leaves in parks within the city centre but increasingly high values for trees located at the roadside.

Several studies have shown the relationship between the distribution of magnetic parameters (e.g. magnetic susceptibility) and heavy metal content (for review, see Petrovsky et al., 1998, Chaparro et al., 2012). The results presented in **Paper III** show significant correlations between magnetic susceptibility and the concentration of selected heavy metals in the case of moss bags exposed to road traffic. The correlation between magnetic parameters and heavy metal content is due to the fact that heavy metals are incorporated into the lattice structure of ferrimagnetic particles during the combustion process or are adsorbed onto the surface of pre-present ferrimagnetics in the environments. The enhanced concentrations of particular heavy metals (e.g. Fe, Mn, Zn, Cu, Cr, Ni and Co) may be associated with specific sources of vehicle emissions (exhaust and non-exhaust emissions) as well as grain size (large active surface of ultrafine particles).

Low-coercivity magnetite was identified as a major magnetic phase in all studied roadside collectors (soil, snow, moss bags and lichens) (**Papers I-IV**). This is indicated by magnetic (e.g., hysteresis, IRM, low and high temperature experiments), micro-morphological (SEM and feature analysis) and mineralogical (Mössbauer, WD-XRF and XRD) analysis. Moreover, magnetic minerals such as titanomagnetite, ilmenite, pyrite and pyrrhotite were observed in the studied samples.

The identified magnetite particles are mostly PSD grains (a mixture of SD (<1 μm) and MD (>10 μm) grains) with a predominant MD fraction (**Papers I-IV**) (Fig. 10). Analysis of street dust from Liverpool by Xie et al. (1999) showed that the main magnetic component is an MD ferrimagnetic phase with a small contribution of SD and antiferromagnetic grains. The higher contribution of coarser magnetic grains in the studied samples might be related to sorting of

particles in the air due to gravity (dry deposition). Larger particles settle at shorter distance from the source, while smaller particles can travel a longer distance from the emission source dependent on wind direction and speed (Zhu et al., 2002). Ultrafine iron oxides (>10 nm) were found in road dust extracted from roadside snow collected at 5 m, 10 m and 15 m distance from the road edge (**Paper IV**). Sagnotti et al. (2006) demonstrated that the magnetic fraction of PM_{10} (particulate matter with an aerodynamic diameter of 10 μm) is a mixture of PSD (natural dust) and superparamagnetic (ultrafine) and MD grains (pollution). The SP fraction is related to exhaust emissions, while the MD fraction may be associated with abrasion of metallic parts. The increased contribution of ultrafine iron-oxides may be associated with increased values of magnetic susceptibility and this can explain the observed deviation (at 15 m) from the decreasing trend of χ with increasing distance from the road (**Paper IV**). The horizontal distribution of SIRM/χ ratio suggests a diminishing grain-size of magnetic particles with increasing distance from the road edge.
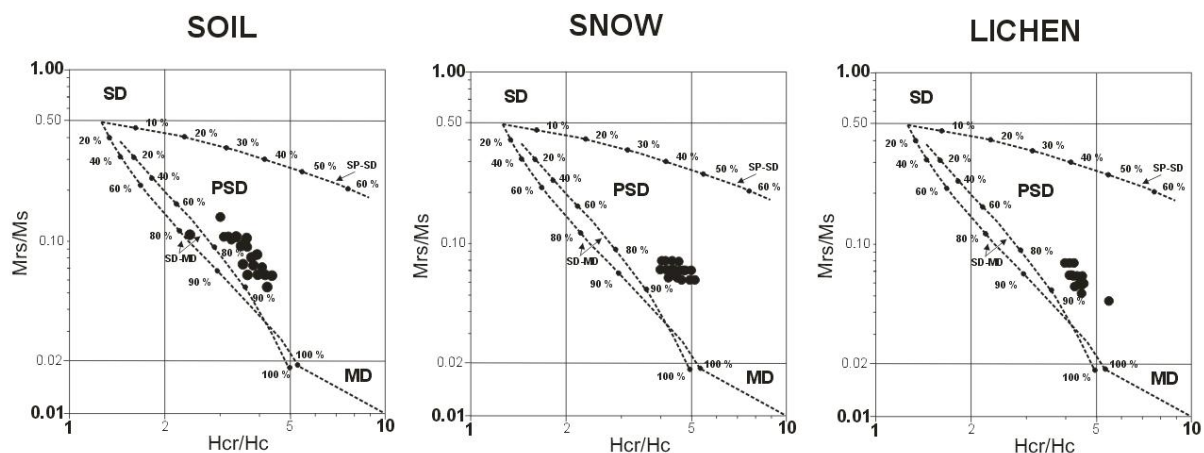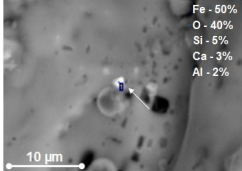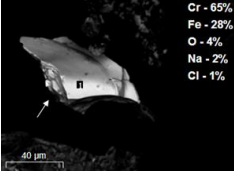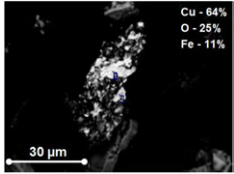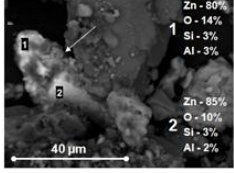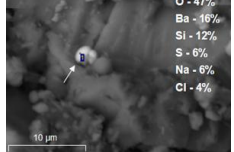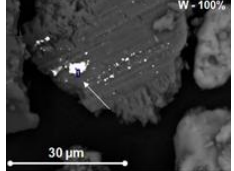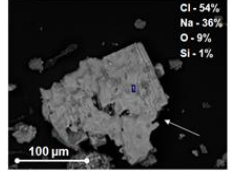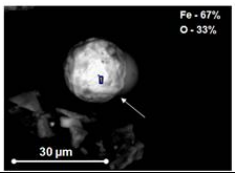

*Figure 10. Day plot of road dust accumulated in roadside soil, snow and lichens sampled near a road. Boundaries for single-domain (SD), pseudo-single-domain (PSD) and multi-domain (MD) grains and mixing lines, indicated by broken lines (SD/MD and SD/superparamagnetic(SP) grains), are shown after Dunlop (2002) (**Papers I-III**).*

Road dust is a mixture of natural and anthropogenic minerals. Resuspended soil and dust produced during weathering of bedrock are sources of minerals such as bastnäsite, uraninite, monazite, zircon, titanomagnetite, ilmenite, pyrite and pyrrhotite (**Papers II, IV**). However,

these minerals may also originate from anthropogenic activities (e.g., abrasion of the road surface) since crushed stone (aggregate), sand and gravel, obtained mostly from local sources, are commonly used for road construction. The sources of particular anthropogenic particles can be discriminated on the basis of their morphological and mineralogical characteristics (Magiera et al., 2011). The examined road dust contains angular and aggregate particles composed of various elements (**Papers I-IV,** Table 6). The grain size and specific chemical composition of each particle may suggest its possible sources. Traffic emissions include particles of different grain sizes such as ultrafine particles (<30 nm, 30-100 nm) formed in the engine, in the exhaust pipe or immediately after the emission; fine particles (0.1-2 μm) formed by chemical reactions or other processes; and coarse mode (>2 μm) generated by abrasion of the road, tyres and brake linings (Palmgren et al., 2003). Since the observed particles are larger than 1 µm, these mainly originate from non-exhaust emissions such as abrasion of vehicle components, road surface and winter road maintenance (Table 6). Furthermore, the studied road dust comprises spherule-shaped particles mostly composed of iron. These are the products of combustion processes e.g. combustion of coal in nearby power plants and/or fuel in vehicle engines.

*Table 6. Anthropogenic particles identified in road dust and their possible sources (Kennedy and Gadd, 2003; Chan and Stachowiak, 2004; Ingo et al., 2004; Birmili et al., 2006; Peltola and Wikström, 2006; Murakami et al., 2007; Thorpe and Harrison, 2008; Sagnotti et al., 2009; Magiera et al., 2011). SEM images and EDS spectrums are taken from **Papers II, IV** and unpublished data.*

Type of particle (grain size):	SEM Image and chemical composition (EDS spectrum)	Major elements identified in the particle	Source
1. Angular/aggregate (~1-300 µm)	Fe - 60% / O - 40% / Si - 5% / Ca - 3% / Al - 2% / 10 µm	Fe, O	Vehicle suspension, brake linings, brake discs, brake callipers and steering knuckles

	Elements	Source
Cr - 65%, Fe - 28%, O - 4%, Na - 2%, Cl - 1%	Cr, Ni, Fe	Road line markings, piston rods in shock absorbers, car door handles, emblems, front grills, wheels, fasteners and engine valves
Cu - 64%, O - 25%, Fe - 11%	Cu	Brake linings
1: Zn - 80%, O - 14%, Si - 3%, Al - 3%; 2: Zn - 85%, O - 10%, Si - 3%, Al - 2%	Zn	Tyre wear, bodywork
O - 47%, Ba - 16%, Si - 12%, S - 6%, Na - 6%, Cl - 4%	Ba, O, S	Brake linings
W - 100%	W	Tyre studs, snowplough components
Cl - 54%, Na - 36%, O - 9%, Si - 1%	Na, K, Cl	de-icing substances
Fe - 67%, O - 33%	Fe, O, Si, Al	burning processes (e.g. coal)

2. Spherules (~1-100 µm)

This study demonstrates that snow is an efficient collector of anthropogenic particles since it can accumulate and preserve the pollutants for several months (until the late stages of melting, **Papers II, IV**). Furthermore, it provides more information about spatial and temporal distribution of contaminants than soil. It is difficult to interpret the data obtained from soil measurements due to its complexity and the effect of underlying geology. This suggests the application of alternative collectors of atmospheric particulates (e.g. snow and

51

moss bags). As shown in **Paper III** moss bags and lichens are well suited for magnetic biomonitoring studies, since they effectively accumulate atmospheric pollution and they can be applied to monitor the spatio-temporal distribution of pollution effects.

This study shows the suitability of various magnetic parameters (concentration and grain-size dependent) in determining the source and spatio-temporal distribution of anthropogenic magnetic particulates and associated heavy metals.

4 Health effects associated with urban air pollution

Traffic-generated emissions are estimated to account for more than 50% of the total emissions of PM in the urban areas of highly industrialized countries (Briggs et al., 1997; Wrobel et al., 2000). These emissions pose serious threats to human health since they are emitted at ground level.

Carbon monoxide (CO) when inhaled affects the bloodstream, reduces the availability of oxygen and can be seriously harmful to public health. Emission of nitrogen dioxide (NO_2) from transport-related sources reduces lung function, affects the respiratory immune defence system and increases the risk of respiratory problems. Emissions of PM from exhaust as well as non-exhaust sources have an impact on air quality in urban areas. The physical and chemical properties of urban particulates are associated with several health risks such as respiratory problems, skin irritation, eye inflammation, blood clotting and various types of allergy. Salonen et al. (2004) found that resuspension particles caused proinflammatory activity in cells due to their endotoxin concentrations and they hypothesized that this might be the reason for irritative symptoms in the respiratory system frequently reported by both asthmatic and healthy people during resuspension episodes. Miguel et al. (1999) reported that road dust contains pollen and other allergens which are capable of causing allergic diseases in humans.

The studied road dust is composed of particles of extremely diverse sizes; from ~10 nm up to 300 µm (**Papers I-IV**). Nanoparticles seem to be generally more toxic than microparticles, mainly due to their ability to penetrate living cells, translocate within the body, and affect the functioning of major organs. Ambient particles cause oxidative stress in biological systems, either directly by introducing oxidant substances, or more indirectly by supplying soluble metals, including transition metals, that shift the redox balance of cells toward oxidation. Oxidative stress is believed to be the primary mechanism by which nanoparticles generate disease (Buzea, 2007). Transition metals, in particular iron, may have adverse effects through non-classical mechanisms such as contributing to the production of hydroxyl radicals through the Fenton reaction (Gilmour et al., 1996). Various heavy metals such as Fe, Cr, Ni, Cu and Zn are emitted into the air in the form of PM with diameters ranging from hundreds of µm down to 1 µm or less (Table 6, **Papers I-IV**). Miguel et al. (1999) found that the relative abundance of Fe, Cu, Zn, Pb and S increased with decreasing particle size. Some of these metals are considered carcinogenic. Long-term exposure to these carcinogens triggers their bioaccumulation in various organs of the body and poses severe health threats (Greene, 2006). The tungsten-rich particles found in the investigated road dust (**Papers II, IV**) are smaller than 2 µm, thus belonging to the respirable size fraction. Few studies exist on the health effects of tungsten-rich particles on the general population, whereas adverse health effects have been identified among people exposed to tungsten in the hard metal industry (Peltola and Wikström, 2006).

References

Angulo, E., 1996. The Tomlinson pollution load index applied to heavy metal "Mussel-Watch" data: a useful index to assess coastal pollution. The *Science of the Total Environment*, **187**, 19–56.

Beckwith, P.R., Ellis, J.B., Revitt, D.M., and Oldfield, F., 1986. Heavy metals and magnetic relationships for urban source sediments. *Physics of the Earth and Planetary Interiors*, **42**, 67–75.

Birmili, W., Allen, A.G., Bary, F., Harrison, R.M., 2006. Trace metal concentrations and water solubility in size-fractionated atmospheric particles and influence of road traffic. *Environmental Science and Technology*, **40**, 1144–1153.

Briggs, D.J., Collins, S., Elliott, P., Ficher. P., Kingham, S., Lebret, E., Pryl, K., van Reeuwijk, H., Smallbone, K., and van der Veen, A., 1997. Mapping urban air pollution using GIS: a regression-based approach. *International Journal of Geographical Information Science*, **11**, 699–718.

Bris, F-J., Garnaud, S., Apperry, N., Gonzalez, A., Mouchel, J-M., Chebbo, G., and Thèvenot, D.R., 1999. A Street Deposit Sampling Method for Metal and Hydrocarbon Contamination Assessment. *The Science of the Total Environment*, **235**, 211–220.

Buzea, C., Pacheco, I.I., and Rombie, K., 2007. Nanomaterials and nanoparticles: Sources and toxicity. *Biointerphases*, **2**, MR17-MR71.

Canagaratna, M.R., Onasch, T.B., Wood, E.C., Herndon, S.C., Jayne, J.T., Cross, E.S., Miake-Lye, R.C., Kolb, C.E., and Worsnop, D.R., 2010. Evolution of vehicle exhaust particles in the atmosphere. *Journal of Air and Waste Management*, **60**, 1192–1203

Canbay, M., Aydin, A., and Kurtulus, C., 2010. Magnetic susceptibility and heavy-metal contamination in topsoils along the Izmit Gulf coastal area and IZAYTAS (Turkey). *Journal of Applied Geophysics*, **70**, 46–57.

Carmichael, R.S. (ed.), 1989. *Practical Handbook of Physical Properties of Rocks and Minerals*. CRC press, Boston, 741 pp.

Chan, D., and Stachowiak, G.W., 2004. Review of automotive brake friction materials. Proceedings of the Institution of Mechanical Engineers Part D. *Journal of Automobile Engineering*, **218**, 953–966.

Chaparro, M.A.E., Marié, D.C., Gogorza, C. S. G., Navas, A.M., and Sinito, A.M., 2010. Magnetic studies and scanning electron microscopy - x-ray energy dispersive spectroscopy analyses of road sediments, soils, and vehicle derived emissions. *Studia Geophysica et Geodetica*, **54**, 633–650.

Chaparro, M.A.E., Chaparro, M.A.E., Sinito, A.M., 2012. An interval fuzzy model for magnetic monitoring: estimation of a pollution index. *Environmental Earth Sciences*, **66**, 1477-1485.

Charlesworth, S.M., and Lees, J.A., 2001. The application of some mineral magnetic measurements and heavy metal analysis for characterising fine sediments in an urban catchment, Coventry, UK. *Journal of Applied Geophysics*, **48**, 113–125.

Day, R., Fuller, M., and Schmidt, V.A., 1977. Hysteresis properties of titanomagnetites: grain size and compositional dependence. *Physics of the Earth and Planetary Interiors*, **13**, 260-267.

Davila, A.F., Rey, D., Mohamed, K., Rubio, B., and Guerra, A.P., 2006. Mapping the sources of urban dust in a coastal environment by measuring magnetic parameters of Platanus hispanica leaves. *Environmental Science and Technolgy*, **40**, 3922–3928.

Dearing, J., 1999, Magnetic Susceptibility. *In:* Walden, Oldfield, J.F., and Smith, J.P., eds., Environmental Magnetism: a practical guide: Technical Guide No. 6, Quaternary Research Association, London, p. 250.

De., Vlieger, I., De., Keukeleere, D., and Kretzschmar, J.G., 2000. Environmental effects of driving behaviour and congestion related to passenger cars. *Atmospheric Environment*, **34**, 4649–4655.

Dekkers, M.J., 2007. Magnetic proxy parameters. *In:* Gubbins, D., and Herrero-Bervera, E., eds., Encyclopedia of Geomagnetism and Palaeomagnetism: Springer, 525–534.

Dunlop, D.J., and Özdemir, Ö., 1997. *Rock magnetism: Fundamentals and Frontiers.* Cambridge University Press, Cambridge, England, 573 pp.

Dunlop, J.D., 2002. Theory and application of the day plot (Mrs/Ms versus Hcr/Hc) 1. Theoretical curves and tests using titanomagnetite data. *Journal of Geophysical Research*, **107**, doi:0.1029/2001JB000486.

El-Hasan, T., 2008. The detection of roadside pollution of rapidly growing city in arid region using the magnetic proxies. *Environmental Geology*, **54**, 23–29.

El-Hasan, T., Al-Nawiseh, A-J., and Lataifeh, M.S., 2009. Environmental Magnetism: Heavy Metal Concentrations in Soils as a Function of Magnetic Materials Content. *Jordan Journal of Earth and Environmental Sciences*, **2**, 38–49.

Ericsson, E., 2000. Variability in urban driving pattern. *Transportation Research Part D*, **5**, 337–354.

Evans, M.E., and Heller, F., 2003, *Environmental Magnetism: Principles and Applications of Enviromagnetics.* International Geophysics Series, v. 86, Academic Press, 299 p.

Finnish Ministry of Transport and Communications, 2005. Environmental guidelines for the transport sector until 2010, 1–37.

Flanders, P.J., 1994. Collection, measurement, and analysis of airborne magnetic particulates from pollution in the environment. *Journal of Applied Physics*, **75**, 5931–5936

Forsberg, B., Hansson, H.C., Johansson, C., Aureskoug, H., Persson, K., and Järvholm, B., 2005. Comparative health impact assessment of local and regional particulate air pollutants in Scandinavia. *Ambio*, **34**, 11–19.

France, D., Hu, Y., Snowball, I., Rolph, T., Oldfield, F., andWalden, J., 1999. Additional rock magnetic measurements. *In:* Walden, J., Oldfield, F., and Smith, J.P., eds., Environmental Magnetism: a practical guide: Technical Guide No. 6, Quaternary Research Association, London, p. 250.

Frey, H.C., Rouphail, N.M., Unal, A., and Colyar, J.D., 2001. Measurement of On-Road Tailpipe CO, NO, and Hydrocarbon Emissions Using a Portable Instrument. *In*: Proceedings of the Annual Meeting of the Air & Waste Management Association, June 24-28. Orlando, FL.

Frey, H.C., Unal, A., Rouphail, N.M., and J. D. Colyar, J.D., 2003. On-road measurement of vehicle tailpipe emissions using a portable instrument. *Journal of Air and Waste Management Association*, **53**, 992–1002.

Gautam, P., Blaha, U., Appel, E., and Neupane, G., 2004. Environmental magnetic approach towards the quantification of pollution in Kathmandu urban area, Nepal. *Physics and Chemistry of the Earth*, **29**, 973–984.

Gautam, P., Blaha, U., and Appel, E., 2005a. Integration of magnetism and heavy metal chemistry of soils to quantify the environmental pollution in Kathmandu, Nepal. *Island Arc*, **14**, 424–435.

Gautam, P., Blaha, U., and Appel, E., 2005b. Magnetic susceptibility of dust loaded leaves as a proxy of traffic-related heavy metal pollution in Kathmandu city, Nepal. *Atmospheric Environment*, **39**, 2201–2211.

Gilmour, P.S., Brown, D.M., Lindsay, T.G., Beswick, P.H., MacNee, W., and Donaldson, K., 1996. Adverse health effects of PM_{10} particles: involvement of iron in generation of hydroxyl radical. *Occupational and Environmental Medicine*, **53**, 817–822.

Goddu, S.R., Appel, E., Jordanova, D., and Wehland, F., 2004. Magnetic properties of road dust from Visakhapatnam (India)-relationship to industrial pollution and road traffic. *Physisc and Chemistry of the Earth*, **29**, 985–995.

Goldstein, J., Newbury, D., Joy, D., Lyman, C., Echlin, P., Lifshin, E., Sawyer, L., and Michael, J., 2003. Scanning electron microscopy and X-ray microanalysis, 3rd ed. New York: Academic/Plenum Publishers.

Greene, N.A., and Morris, V.R., 2006. Assessment of Public Health Risks Associated with Atmospheric Exposure to $PM_{2.5}$ in Washington, DC, USA. *International Journal of Environmental Research and Public Health*, **3**, 86–97.

Hanesch, M., and Scholger, R., 2002. Mapping of heavy metal loadings in soils by means of magnetic susceptibility measurements. *Environmental Geology*, **42**, 857–870.

Hoffmann, V., Knab, M., Appel, E., 1999. Magnetic susceptibility mapping of roadside pollution. *Journal of Geochemical Exploration*, **66**, 313–326.

Hopke, P.K., Lamb, R.E., and Natusch, F.S., 1980. Multielemental characterization of urban roadway dust. *Environmental Science and Technolgy*, **14**, 164–175.

Hounslow, M., and Maher, B., 1999. Laboratory procedures for quantitative extraction and analysis of magnetic minerals from sediments: *In* J. Walden, F. Oldfield, and J. P. Smith, eds., Environmental Magnetism: a practical guide: Technical Guide No. 6, Quaternary Research Association, London, p. 250.

Hrouda, F., Muller, P., and Hanak, J., 2003. Repeated progressive heating in susceptibility vs. temperature investigation: a new paleotemperature indicator?: *Physics and Chemistry of the Earth*, **28**, 653–657.

Ingo, G.M., D'uffizi, M., Falso, G., Bultrini, G., and Padeletti, G., 2004. Thermal and microchemical investigation of automotive brake pad wear residues. *Thermochimica Acta*, **418**, 61–68.

Jordanova, D., Petrov, P., Hoffmann, V., Gocht, T., Panaiotu, C., Tsacheva, T., Jordanova, N., 2010. Magnetic signature of different vegetation species in polluted environment. *Studia Geophysica et Geodaetica*, **54**, 417–442

Kauhaniemi, M., 2003. Usability of the Air Quality Model CAR-FMI in City Planning. Master's Thesis, University of Oulu, Department of Process and Environmental Engineering, Control Engineering Laboratory, 87+7 (13) p.

Kennedy, P., and Gadd, J., 2003. Preliminary examination of trace elements in tyres, brake pads, and road bitumen in New Zealand. Prepared for Ministry of transport, New Zealand.

Ketzel, M., Omstedt, G., Johansson, C., During, I., Pohjola, M., Oettl, M., Gidhagen, L., Lohmeyer, A., Berkowicz, R., and Wĺhlin, P., 2007. Estimation and validation of $PM_{2.5}/PM_{10}$ exhausted and non-exhausted emission factors for practical street pollution modelling. *Atmospheric Environment*, **41**, 9370–9385.

Kerminen, V.M., Mäkelä, T.E., Ojanen, C.H., Hillamo, R.E., Vilhunen, J.K., Rantanen, L., Havers, N., VonBohlen, A., and Klockow, D., 1997. Characterization of the particulate phase in the exhaust from a diesel car. *Environmental Science and Technology*, **31**, 1883–1889.

Kim, W., Doh, S.J., Park, Y.H., and Yun, S.T., 2007. Two-year magnetic monitoring in conjunction with geochemical and electron microscopic data of roadside dust in Seoul, Korea. *Atmospheric Environment*, **41**, 7627–7641.

Kim, W., Doh, S-J., and Yu, Y., 2009. Anthropogenic contribution of magnetic particulates in urban roadside dust. *Atmospheric Environment*, **43**, 3137–3144.

Kittelson, D., Johnson, J., Watts, W., Wei, Q., Drayton, M., Paulsen, D., and Bukowiecki, N., 2000. Diesel aerosol sampling in the atmosphere, Society of Automotive Engineers (SAE) Technical Paper 2000-01-2212; SAE: Warrendale, PA.

Kletetchka, G., Žila, V., and Wasilewski, P.J. 2003. Magnetic anomalies on the tree trunks. *Studia Geophysica et Geodaetica*, **47**, 371–379.

Kuhns, H., Etyemezian, V., Green, M., Hendrickson, K., McGown, M., Barton, K., and Pitchford, M., 2003. Vehicle-based road dust emission measurement - Part II: Effect of

precipitation, wintertime road sanding, and street sweepers on inferred PM_{10} emission potentials from paved and unpaved roads. *Atmospheric Environment*, **37**, 4573–4582

Kupiainen, K., 2007. Road dust from pavement wear and traction sanding. Monographs of the Boreal Environment Research, 26, 50.

Leśniewska, B.A., Messerschmidt, J., Jakubowski, N., Hulanicki, A., 2004. Bioaccumulation of platinum-group elements and characterization of their species in Lolium multiflorum by size-exclusion chromatography coupled with ICP-MS. *Science of The Total Environment*, **322**, 95-108.

Lin, C.C., Chen, S.J., Huang, K.L., Hwang, W.I., Chang-Chien, G.P. and Lin, W.Y., 2005. Characteristics of metals in nano/ultrafine/fine/coarse particles collected beside a heavily trafficked road. *Environmental Science and Technology*, **39** (21), 8113−8122.

Lough, G.C., Schauer, J.J., Park, J.-S., Shafer, M.M., Deminter, J.T., and Weinstein, J.P., 2005. Emissions of metals associated with motor vehicle roadways. *Environmental Science and Technology*, **39**, 826–836.

Lu, S.G., Bai, S.Q., Cai, J.B., and Xu, C., 2005. Magnetic properties and heavy metal contents of automobile emission particulates. *Journal of Zhejiang University Science B*, **6**, 731–735.

Lu, S.G., and Bai, S.Q., 2006. Study on the correlation of magnetic properties and heavy metals content in urban soils of Hangzhou city, China. *Journal of Applied Geophysics*, **60**, 1–12.

Lu, S.G., Bai S.Q., and Xue Q.F., 2007. Magnetic properties as indicators of heavy metals pollution in urban topsoils: case study from the city of Luoyang, China. *Geophysical Journal International*, **171**, 568-580.

Magiera, T., Jabłońska, M., Strzyszcz, Z., and Rachwał, M., 2011. Morphological and mineralogical forms of technogenic magnetic particles in industrial dusts. *Atmospheric Environment*, **45**, 4281–4290.

Maher, B., 1986. Characterization of soils by mineral magnetic measurements. *Physics of the Earth and Planetary Interiors*, **42**, 76–92.

Maher, B.A., Moore, C., Matzka, J., 2008. Spatial variation in vehicle-derived metal pollution identified by magnetic and elemental analysis of roadside tree leaves. *Atmospheric Environment*, **42**, 364–373.

Marié, D.C., Chaparro, M.A.E., Gogorza, C.S.G., Navas, A., and Sinito, A.M., 2010. Vehicle-derived emissions and pollution on the road Autovia 2 investigated by rock-magnetic parameters: a case of study from Argentina, *Studia Geophysica et Geodaetica*, **54**, 135–152.

Mathissen, M., Scheer,V., Vogt, R., and Benter, T., 2011. Investigation on the potential generation of ultrafine particles from the tire-road interface. *Atmospheric Environment*, **45**, 6172–6179.

Mathissen, M., Scheer, V., Kirchner, U., Vogt, R., and Benter, T., 2012. Non-exhaust PM emission measurements of a light duty vehicle with a mobile trailer, *Atmospheric Environment*, doi: 10.1016/j.atmosenv.2012.05.020

Matzka, J., and Maher, B.A., 1999. Magnetic biomonitoring of roadside tree leaves: identification of spatial and temporal variations in vehicle-derived particulates. *Atmospheric Environment*, **33**, 4565–4569.

McIntosh, G., Gomez-Paccard, M. and Osete, M. L., 2007. The magnetic properties of particles deposited on Platanus x hispanica leaves in Madrid, Spain, and their temporal and spatial variations. *Science of The Total Environment*, **382**, 135–146.

Miguel, A.G., Cass, G.R., Glovsky, M.M., and Weiss, J., 1999. Allergens in Paved Road Dust and Airborne Particles. *Environmental Science and Technology*, **33**, 4159–4168.

Mitchell, R., and Maher, B.A., 2009. Evaluation and application of biomagnetic monitoring of traffic-derived particulate pollution. *Atmospheric Environment*, **43**, 2095–2103.

Morawska, L., (Jim) Zhang J., 2002. Combustion sources of particles. 1. Health relevance and source signatures. *Chemosphere*, **49**, 1045–1058.

Moreno, E., Sagnotti, L., Dinares-Turell, J., Winkler, A., Cascella, A., 2003. Biomonitoring of traffic air pollution in Rome using magnetic properties of tree leaves. *Atmospheric Environment*, **37**, 2967–2977.

Morris, W.A., Versteeg, J.K., Bryant, D.W., Legzdins, A.E., McCarry, B.E., and Marvin, X.H., 1995. Preliminary comparisons between mutagenic and magnetic susceptibility of respirable airborne particle. *Atmospheric Environment*, **29**, 3441–3450.

Murakami, M., Nakajima, F., Furumai, H., Tomiyasu, B., and Owari, M., 2007. Identification of particles containing chromium and lead in road dust and soakaway sediment by electron probe microanalyser. *Chemosphere*, **67**, 2000–2010.

Muxworthy, A., Matzka, J., and Petersen, N., 2001. Comparison of magnetic parameters of urban atmospheric particulate matter with pollution and meteorological data. *Atmospheric Environment*, **35**, 4379–4386.

Muxworthy, A., Schmidbauer, E., and Petersen N., 2002. Magnetic properties and Mossbauer spectra of urban atmospheric particulate matter, a case study from Munich, Germany. *Geophysical Journal International*, **150**, 558–570.

Muxworthy, A.R., Matzka, J., Davila, A.F., and Peterson, N., 2003. Magnetic signature of daily sampled urban atmospheric particles. *Atmospheric Environment*, **37**, 2967–77.

Myung, C.L., and Park, S., 2012. Exhaust nanoparticle emissions from internal combustion engines: A review. *International Journal of Automotive Technology*, 13, 9–22.

Ng, S.L., Chan, L.S., Lam, K.C. and Chan, W.K., 2003. Heavy metal contents and magnetic properties of playground dust in Hong Kong. *Environmental Monitoring and Assessment*, **89**, 221–232.

Nicholson, K.W., and Branson, J.R., 1990. Factors affecting resuspension by road traffic. *The Science of the Total Environment*, **93**, 349–358.

Olson, K.W., and Skogerboe, R.K., 1975. Identification of soil lead compounds from automotive sources. *Environmental Science and Technology*, **9**, 227–230.

Omstedt, G., Bringfelt, B., and Johansson, C., 2005. A model for vehicle-induced nontailpipe emissions of particles along Swedish roads. *Atmospheric Environment*, **39**, 6088–6097.

Palmgren, F., Waahlin, P., Kildesó, J., Afshari, A., and Fogh, C.L., 2003. Characterisation of particle emissions from the driving car fleet and the contribution to ambient and indoor particle concentrations. *Physics and Chemistry of the Earth*, **28**, 327–334.

Peltola, P., and Wikström E., 2006. Tyre stud derived tungsten carbide particles in urban street dust. *Boreal Environment Research*, **11**, 161–168.

Peters, C., and Dekkers, M.J., 2003. Selected room temperature magnetic parameters as a function of mineralogy, concentration and grain size. *Physics and Chemistry of the Earth*, **28**, 659-667.

Petrovsky, E., Kapicka, A., Zapletal, K., Sebestova, E., Spanila, T., Dekkers, M.J., and Rochette, P., 1998. Correlation between magnetic parameters and chemical composition of lake sediments from northern Bohemia - preliminary study. *Physics and Chemistry of the Earth*, **23**, 1123–1126.

Pope, C.A., Burnett, R.T., Thun, M.J., Calle, E.E., Krewski, D., Kazuhiko, I., and Thurston, G.D., 2002. Lung cancer, cardiopulmonary mortality, and long-term exposure to fine particulate air pollution. *Journal of the American Medical Association*, **287**, 1132–1141.

Pope, C.A., and Dockery, D.W., 2006. Health effects of fine particulate air pollution: lines that connect. *Journal of the Air and Waste Management Association*, **56**, 709–742.

Pöschl, U., 2005. Atmospheric aerosols: Composition, transformation, climate and health effects. *Angewandte Chemie International Edition*, **44**, 7520–7540.

Roberts, A.P., Pike, C.R., and Verosub, K.L., 2000. First-order reversal curve diagrams: A new tool for characterizing the magnetic properties of natural samples. *Journal of Geophysical Research*, **105**, 28,461–28,475.

Robertson, D.J., Taylor, K.G., Hoon, S.R., 2003. Geochemical and mineral magnetic characterisation of urban sediment particulates, Manchester, UK. *Applied Geochemistry*, **18**, 269–282.

Sagnotti, L., Macrí, P., Egli, R., and Mondolio, M., 2006. Magnetic properties of atmospheric particulate matter from automatic air sampler stations in Latium (Italy): towards a definition of magnetic fingerprints for natural and anthropogenic PM_{10} sources. *Journal of Geophysical Research*, **111**, B12S22

Sagnotti, L., Taddeucci, J., Winkler, A., and Cavallo, A., 2009. Compositional, morphological, and hysteresis characterization of magnetic airborne particulate matter in

Rome, Italy. *Geochemistry, Geophysics, Geosystems*, **10**, Q08Z06, doi:10.1029/2009GC002563.

Salonen, R.O., Halinen, A.I., Pennanen, A.S., Hirvonen, M.-R., Sillanpaa, M., Hillamo, R., Shi, T., Borm, P., Sandell, E., Koskentalo, T., and Aarnio, P., 2004. Chemical and in vitro toxicologic characterization of wintertime and springtime urban-air particles with an aerodynamic diameter below 10 μm in Helsinki . *Scandinavian Journal of Work, Environment and Health*, **30**, 80–90.

Shilton, V.F., Booth, C.A., Smith, J.P., Giess, P., Mitchell, D.J., and Williams, C.D., 2005. Magnetic properties of urban street dust and their relationship with organic matter content in the West Midlands, UK. *Atmosphercic Environment*, **39**, 3651–3659.

Szönyi, M., Sagnotti, L., and Hirt, A.M., 2008. A refined biomonitoring study of airborne particulate matter pollution in Rome, with magnetic measurements of Quercus Ilex tree leaves. *Geophysical Journal International*, **173**, 127–141.

Singh, A.K., Hasnain, S.I., and Banerjee, D.K., 2003. Grain size and geochemical portioning of heavy metals iin sediments of the Danodar River e a tributary of the lower Ganga, India. *Environmental Geology*, **39**, 90–98.

Sioutas, C., Delfino, R.J., and Singh, M., 2005. Exposure assessment for atmospheric ultrafine particles (UFPs) and implications in epidemiologic research. *Environmental Health Perspectives*, **113**, 947–955

Spassov, S., Egli, R., Heller, F., Nourgaliev, D.K., and Hannam, J., 2004. Magnetic quantification of urban pollution sources in atmospheric particulate matter. *Geophysical Journal International*, **159**, 555–64.

Sternbeck, J., Sjödin, Å., and Andréasson, K., 2002. Metal emissions from road traffic and the influence of resuspension—results from two tunnel studies. *Atmospheric Environment*, **36**, 4735–4744.

Thompson, R., and Oldfield, F., 1986. *Environmental Magnetism*. Allen and Unwin, London. 1–227.

Thorpe, A., and Harrison, R.M., 2008. Sources and properties of non-exhaust particulate matter from road traffic: a review. *Science of the Total Environment*, **400**, 270–282.

Urbat, M., Lehndorff, E., and Schwark, L., 2004. Biomonitoring of air quality in the Cologne conurbation using pine needles as a passive sampler — Part 1: Magnetic properties. *Atmospheric Environment*, **38**, 3781–92.

Vaze, J., and Chiew, H.S., 2002. Experimental study of pollutant accumulation on an urban road surface. *Urban Water*, **4**, 379–389.

Winklhofer, M., and Zimanyi, G.T., 2006. Extracting the intrinsic switching field distribution in perpendicular media: a comparative analysis. *Journal of Applied Physics*, **99**, doi:10.1063/1.2176598 08E710-1-3.

Wróbel, A., Rokita, E., and Maenhaut, W., 2000. Transport of traffic-related aerosols in urban areas. *Science of the Total Environment*, **257**, 199–211.

Xie, S., Dearing, J.A., and Bloemendal, J., 1999a. A partial susceptibility approach to analysing the magnetic properties of environmental materials: a case study. *Geophysical Journal International*, **138**, 851–856.

Xie, S., Dearing, J.A., Bloemendal, J., and Boyle, J.F., 1999b. Association between the organic matter content and magnetic properties in street dust, Liverpool, UK. *Science of the Total Environment*, **241**, 205–214.

Xie, S., Dearing, J.A., and Bloemendal, J., 2000. The organic matter content of street dust in Liverpool, UK, and its association with dust magnetic properties. *Atmospheric Environment*, **34**, 269–275.

Xie, S., Dearing, J.A., Boyle, J.F., Bloemendal, J., and Morse, A.P. 2001. Association between magnetic properties and element concentrations of Liverpool street dust and its implications. *Journal of Applied Geophysics*, **48**, 83–92.

Yang, T., Liu, Q., Chan, L., and Cao, G., 2007. Magnetic investigation of heavy metals contamination in urban topsoils around the East Lake, Wuhan, China. *Geophysical Journal International*, **171**, 603–612.

Yang, T., Liu, Q., Li, X., Zeng, Q., and Chan, L., 2010. Anthropogenic magnetic particles and heavymetals in the roaddust: Magnetic identification and its implications. *Atmospheric Environment*, **44**, 1175–1185.

Zhang, K.M., Anthony, S., and Wexlera, A.S., 2004. Evolution of particle number distribution near roadways - Part I: Analysis of aerosol dynamics and its implications for engine emission measurement. *Atmospheric Environment*, **38**, 6643–6653.

Zhu, Y., Hinds, W.C., Kim, S., and Sioutas, C., 2002. Concentration and size distribution of ultrafine particles near a major highway. *Journal of the Air and Waste Management Association*, **52**, 1032–1042.